Evolution and Enabling Capabilities of Spatially Resolved Techniques for the Characterization of Heterogeneously Catalyzed Reactions

ACS Catalysis

Perspective

pubs.acs.org/acscatalysis

Evolution and Enabling Capabilities of Spatially Resolved Techniques for the Characterization of Heterogeneously Catalyzed Reactions

Kevin Morgan,*[,†] Jamal Touitou,[‡] Jae-Soon Choi,[§] Ciarán Coney,[∥] Christopher Hardacre,[∥] Josh A. Pihl,[§] Cristina E. Stere,[∥] Mi-Young Kim,[§] Caomhán Stewart,[∥] Alexandre Goguet,*[,∥] and William P. Partridge*[,§]

[†]School of Mechanical and Aerospace Engineering, Queen's University Belfast, Ashby Building, Stranmillis Road, Belfast BT9 5AH, United Kingdom

[‡]Department of Chemical and Materials Engineering, King Abdulaziz University, Jeddah, Saudi Arabia

[§]Fuels, Engines and Emissions Research Center, Oak Ridge National Laboratory, P.O. Box 2008, MS-6472, Oak Ridge, Tennessee 37831-6472, United States

[∥]School of Chemistry and Chemical Engineering, Queen's University Belfast, David Keir Building, Stranmillis Road, Belfast BT9 5AG, United Kingdom

ABSTRACT: The development and optimization of catalysts and catalytic processes requires knowledge of reaction kinetics and mechanisms. In traditional catalyst kinetic characterization, the gas composition is known at the inlet, and the exit flow is measured to determine changes in concentration. As such, the progression of the chemistry within the catalyst is not known. Technological advances in electromagnetic and physical probes have made visualizing the evolution of the chemistry within catalyst samples a reality, as part of a methodology commonly known as spatial resolution. Herein, we discuss and evaluate the development of spatially resolved techniques, including the evolutions and achievements of this growing area of catalytic research. The impact of such techniques is discussed in terms of the invasiveness of physical probes on catalytic systems, as well as how experimentally obtained spatial profiles can be used in conjunction with kinetic modeling. Furthermore, some aims and aspirations for further evolution of spatially resolved techniques are considered.

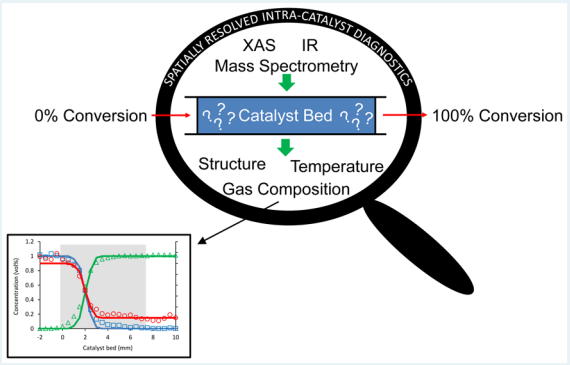

KEYWORDS: *spatial resolution, catalyst characterization, monoliths, packed beds, electromagnetic probes, physical probes*

1. INTRODUCTION

Measurements are a critical and enabling aspect of understanding, developing, optimizing, and modeling catalytic processes. Advanced techniques capable of measuring spatial and temporal reaction distributions within a catalyst during realistic operating conditions provide leap-scale benefits over conventional integral measurements with respect to advancing catalysis. The goal of this work is to review the development, application, and the state-of-the-art advances of such techniques for *operando* spatiotemporally resolved intracatalyst characterization and to consider the invasive nature of these techniques, describe specific methods for quantifying invasive nature, and summarize the impact of these techniques for advancing catalyst knowledge and modeling. It is the hope that this work will be useful in providing a historical perspective on the development of intracatalyst analysis, insights into their potential for advancing catalytic research and development, and specific guidance for experimental design incorporating these enabling measurement techniques. The various sections are summarized here to give an overview of the work and guide the reader.

A brief summary of the importance of catalysis and catalysts, as well as some insight into the catalytic development process are reported in Section 2. Section 3 discusses traditional methods for catalyst characterization based on integral or effluent measurements; the inherent limitations of these approaches are discussed, which provides a foundation for the motivation and need for spatially resolved *operando* intracatalyst measurements. Spatially resolved techniques are discussed in Section 4, which is divided into two sections focusing on those using electromagnetic and physical probes. The section on electromagnetic probes covers a wide range of techniques including spectroscopic and imaging methodologies. Electromagnetic probes are predominantly sensitive to the state of the catalyst, but IR and MRI can be used to measure reactant and product concentrations in a limited number of situations, such as liquid-phase catalysis. While electromagnetic probes can be completely noninvasive, their applications are not always such,

Received: November 18, 2015
Revised: January 11, 2016
Published: January 15, 2016

DOI: 10.1021/acscatal.5b02602
ACS Catal. 2016, 6, 1356−1381

and they should not be considered universally superior to physical probes; for example, with electromagnetic sources of high brilliance and/or energy density, there is always the possibility that the sample could be irreversibly altered, thereby obfuscating meaningful structure−activity relationship determinations. Furthermore, the nature of some electromagnetic-based techniques can limit their spatial resolution (e.g., line-of-sight absorption wherein the resultant measurement is based on the integral of many interactions along the probe-beam's path, which are not individually resolved). While electromagnetic probes can provide spatial resolution in some applications (e.g., tomography), the required optical access may not be practically achievable without compromising the natural state of the reactor (at least two points of optical access required, on opposite sides of reactor) and thus becoming invasive.

The principal advantages of physical probes are that they more directly provide spatial resolution (predominantly, although not exclusively, for the gas phase) and can require fewer changes to the natural reactor state for measurement access. The section on physical probes is the primary focus of this work and specifically discusses Spaci-MS, IR Imaging, Spaci-IR, and techniques using optical fibers including pyrometry, phosphor thermography, Raman and optical frequency domain reflectometry, as well as applications to powder-bed, honeycomb-, and foam-monolith-supported catalysts. Related discussion addresses and compares different approaches to balancing the trade-offs between temporal resolution, spatial resolution, and invasive nature. Section 5 describes numerical, experimental, and dimensionless-factor methodologies for assessing the invasive nature of physical sampling probes like those used for Spaci-MS and shows that these can be practically noninvasive in a wide range of applications. Section 6 reports the enabling capabilities of spatially resolved techniques for the enhancement of kinetic modeling, as this has been discussed for a range of techniques and processes. Section 7 is the culmination of the previous sections, highlighting the major points while some aims and aspirations for further evolution of spatially resolved techniques are considered.

2. CATALYSIS AND CATALYSTS

Catalysis plays an important role in the chemical industry, both economically and environmentally. For example, between 75%[1] and 80%[2] of products from all industrial sectors (such as polymers, pharmaceuticals, agrochemicals, petrochemicals, and environmental cleanup) involve the use of catalysis at some point. For the general public, the best-known example of catalysis is probably the catalytic converter used by the automotive industry for emission control. It is also well-understood that without the use of catalysts, some reactions will occur with very slow kinetics, if even at all. One of the alternatives to improve reaction kinetics is to increase the temperature and/or pressure in order to increase the rate of conversion. These can lead to severe conditions with subsequent undesirable increased energy consumption but can also cause extreme damage to instruments and materials (corrosion and stress leading to a higher level of maintenance). Another reason to use catalysts is to increase the selectivity toward a desired product which also reduces waste of reactants due to side reactions. The use of catalysts can allow chemical reactions to occur under less-severe temperatures and/or pressures, with a greater selectivity, with a better conversion, and at a higher rate.[1−4]

Catalysts can be found in different shapes and forms depending on the stage of development and the final application. In academia, and at the early stage of industrial research, the most common form will be a powder because it is the easiest form to prepare and to model as it presents fewer problems in terms of heat and mass transfer. In a more advanced stage of research (pilot plant) or for commercialized catalyst used in the industry, the shape will preferably be pellets, tablets, rings, spheres, or monoliths, depending on the requirements of the end use.

The development of these commercialized catalysts is the result of combined research in various fields including catalytic activity, kinetics, materials properties, and process engineering. The evaluation of a catalyst for an industrial process is mainly based on economic considerations which generally correspond to the catalyst providing the best compromise between conversion, selectivity, mildest reaction conditions, stability, and lifetime.

Every catalyst goes through an optimization process which generally lasts an average of 5 years from the start of a project to the commercialization.[4] Even after this process, the catalyst can still be improved. Excluding the improvement of the physical aspects of the catalyst during the reaction (elements which depend on material and process engineering), the chemical properties can also be enhanced. Catalyst optimization is possible only with a good understanding of the phenomena occurring at the catalyst surface (under working conditions) and within the reactor. To extract such information, the catalyst needs to be investigated by two avenues available to catalytic research and which are complementary to one another; the first is kinetic characterization, and the second is the physical characterization of the catalyst.

3. TRADITIONAL APPROACHES TO CATALYST KINETIC AND PHYSICAL CHARACTERIZATION

In order to achieve optimal developments of gas-phase heterogeneously catalyzed continuous processes, an in-depth understanding of the kinetics of surface reactions is critical, especially when using complex reactant mixtures.[5] The conventional test is simple, whereby the catalyst is loaded in a reactor within which the pressure and the temperature are controlled, with the reaction gas mixture flowing through the reactor. The gas is then sampled and analyzed at the outlet of the reactor to determine its composition using different techniques, for example, by gas chromatography (GC), Fourier Transform Infrared (FTIR) spectroscopy or mass spectrometry (MS). This method of analysis is known as integral, "tail pipe end," or "catalyst effluent" analysis,[6,7] which the majority of experimental kinetic studies, to date, have used. To access kinetics information, the conditions of the reactions in terms of reactants' concentration, reactor temperature, space velocity, and pressure are varied, and the catalyst performance in terms of end-pipe measurement is monitored. Subsequently, mechanistic models with derived kinetics equations (which may or may not take into account additional aspects such as thermodynamics or reactor geometry considerations) are postulated and their output (usually after some degree of tuning of the kinetics parameters) compared to the experimental data to evaluate and rank the validity of the postulated models. While this approach gives a global overview of the activity of the catalyst and possible kinetics models, it does not allow access to information regarding the evolution of the kinetics as a function of the changing gas composition within a catalyst (i.e., with the

DOI: 10.1021/acscatal.5b02602
ACS Catal. 2016, 6, 1356−1381

progressive buildup and possible intracatalyst consumption of the products and selective removal of reactants). This information is important because the vast majority of the postulated kinetics models will have more than one set of kinetics parameters which appear to accurately model the experimentally measured integral performance. That, of course, is already assuming that the model itself does capture properly the chemistry taking place in the reactor. This latter point is crucial and is far from being an easy task. Being able to access the maximum possible information in terms of where the various reactions occur within the reactor to assist the mechanistic construction is essential. It should be noted that such intrareactor information will also help constraining the model and drastically reduce the number of sets of kinetics parameters needed to develop a robust catalyst model which can accurately match experimentally measured spatiotemporal performance.

This lack of information from the tail-pipe approach on the chemical process within the catalyst bed is a consequence of the limits of tail-pipe-end/catalyst-effluent techniques currently used for analysis. As previously mentioned, these techniques (e.g., MS, FTIR and GC) are based on having a probe located at the reactor end (downstream of the catalyst bed) to sample the exit flow of the gases. Figure 1 represents a typical system

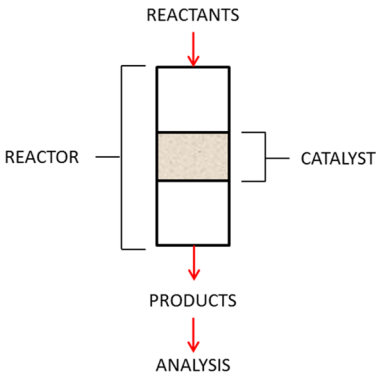

Figure 1. Principle of end-pipe sampling. The reactant concentrations are known, and after formation, products exit the reactor and product concentrations are determined using analytical methods, for example, mass spectrometry or chromatography.

with the reactants introduced into the reactor, continuing flow through the catalyst bed (where the reaction occurs) and subsequent analysis of the reactor effluent flow downstream of the catalyst bed. The only information that can be extracted is the difference of concentration between the inlet (known) and the outlet (measured). Unfortunately, the real point of interest in catalysis research is actually within the catalyst bed itself. In end-pipe sampling analytical methods, the catalyst bed is seen as a "black box" as the techniques do not have direct access to the chemistry occurring within the catalyst bed (interaction between the reactants and the catalyst).

Physical characterization of the catalyst focuses on the chemical nature and structure of the catalyst. Numerous techniques have been developed and are available to measure these characteristics; these techniques are based on different principles including spectroscopy, microscopy, and probe molecules and can provide a large variety of information on the catalyst. The most common characterization techniques which have been utilized to provide analysis of the length and/or breadth of catalytic reactors are the following:[4]

X-ray diffraction (XRD)
X-ray absorption spectroscopy (XAS)/fine structure (XAFS)/near edge (XANES)
infrared spectroscopy (IR)
Raman spectroscopy
ultraviolet spectroscopy (UV)
electron microscopy (SEM, TEM)
nuclear magnetic resonance/magnetic resonance imaging (NMR/MRI)

Not all these techniques are used during catalyst characterization due to the specificity and nature of sample environment of each, but usually, a number of the techniques are combined to gather as much data to support the characterization.[8−20] However, most of these characterization techniques are typically not conducted under true reaction conditions, and some of the techniques are even the subject of debate concerning the information obtained and whether it can be transferred to real life catalysts under real working conditions.[5,21]

To address this issue, new approaches are continually being developed which aim to study real catalysts under optimum conditions as close as possible to real industrial reaction conditions, recently termed as *operando* techniques. Some techniques have already been developed with *operando* modes, including XRD,[14,22] XAFS,[13,23] and diffuse reflectance infrared fourier transform spectroscopy (DRIFTS).[8,9,24] Each characterization technique has its own limitations, and for this reason, in recent years, the approach to catalyst investigation has been developed to enable combinations of these techniques to be used at the same time.[8,20,25] The motivation for this is to simultaneously extract as much information as possible from the catalytic material, ideally using an *operando* system.

In the case of catalyst characterization, an additional issue is present, the impact and origin of which are closely interwoven with the kinetics characterization. During the catalytic process, the population of adsorbed species on the surface of the catalyst evolves with the reaction conditions and catalyst structure. In return, it is today widely recognized that the structure of the catalyst can be modified by the nature of the reaction environment and the adsorbed species. If a plug flow reactor is used (which is very often the case), two situations are possible:

(1) The reactor is used under integral conditions (i.e., high conversions)

This implies that the concentration of reactants and products changes significantly between the inlet and outlet of the reactor. This has two impacts: First the end-pipe data cannot be used to directly extract reaction rates (theoretically, in such cases, the reactions have infinity of reaction rates between the inlet and outlet of the reactor). Second, if the catalyst structure and concentration of the surface species depend on the chemical environment, they will change significantly from inlet to outlet. Consequently, unless intracatalyst spatially resolved characterization is performed, it is not possible to relate the structural data and surface characterization to activity/selectivity.

(2) The reactor is under differential conditions (i.e., low conversions)

In this case, the concentration gradient across the reactor is considered negligible, and the environment is assumed to be homogeneous across the catalyst bed. It is, therefore, possible to calculate reaction rates from

DOI: 10.1021/acscatal.5b02602
ACS Catal. 2016, 6, 1356−1381

activity data and assume that the structure is homogeneous along the bed. The main issue with such an approach is that the low conversion conditions are not representative of the true conditions that the catalyst will experience when operating industrially. Moreover, it is important to be conscious that the types and concentrations of surface species[26,27] as well as the structure of the catalyst (for example, metal particle size)[28] are dependent on the chemical environment. Consequently, these differential conditions will only represent a very narrow "range" of the "environment versus structure" dependence, and structure/activity/selectivity relationships derived from such a narrow range can have very limited applicability in broader applications outside the narrow analysis range.

As discussed earlier, kinetic data and reaction modeling can be used to improve the understanding of phenomena occurring in the catalyst bed, and prediction of catalyst behavior obtained via simulation is highly desirable. For that reason, simple and complex models based on experimentally derived kinetic information have been developed (see Section 6 for more details). Such simulations show an interesting advantage as it is possible to estimate the evolution of reactions within the catalytic reactor under real operating conditions at a limited cost. However, most models are only applicable to very specific conditions, which can limit the broader development for real applications. Another problem with the traditional approach is that model predictions of the evolutions of reactions within the catalyst bed cannot be validated by integral experiments due to the previously outlined limits of such experimental analysis techniques.[29] Therefore, a complete understanding of the overall reaction process cannot be obtained using the integral or catalyst-effluent techniques.

Beyond needing to access sufficiently detailed and accurate intracatalyst reaction-profile data, there are limitations associated with the current state-of-the-art catalytic-monolith models,[30,31] being based almost entirely on global kinetics. The major drawback of this approach is the limited predictive capabilities of such global-kinetics models.[32] The intrinsic kinetics (also known as microkinetics) approach offers much more information about the processes occurring within the catalytic reactor but is significantly more complex and time-consuming to develop.[33,34]

Another aspect that needs consideration in modeling is the determination of appropriate kinetic parameters. Given the number and interdependence of reactions, the process of manually determining the optimum set of kinetic parameters is becoming increasingly challenging. This obviously requires a degree of trial and error in the complex fitting of multidimensional parameters as part of the optimization process, and it is, therefore, a labor-intensive process that requires expert knowledge in a number of areas, for instance, the elementary steps of reactions. Moreover, a simple manual approach is vulnerable to identifying kinetic values in a local optimum, which may not represent the best overall fit to broader experimental data and therefore provide incorrect kinetic parameter sets. Optimization algorithms can ensure that the entire design space is considered in the evaluation, thereby reducing the risk of determining local rather than global optima. Ultimately, an optimizer should reduce the time required to develop a broadly applicable and reliable model of a new catalyst formulation.[35] This aspect, while very important, is beyond the scope of this review, and interested readers can find further information in the papers cited in ref 35.

While traditional methods, including modeling, to measure physical and kinetic characteristics of catalytic systems have been useful, the understanding of the phenomena occurring within the packed bed inside the reactor is limited. For instance, the physical characterization tends to take place at a fixed point and/or depth (in spectroscopy, for example) or via sampling probes located outside of and downstream of the catalyst. Similarly, theoretical models are applicable for a limited number of reactions, giving a global overview for only very specific conditions (pressure, flow rate, gas composition, and temperature). In general, it has not been possible to conduct in depth experimental validation of such models due to limitations of gas sampling within the catalyst system. Recent technical developments (herein referred to as spatial resolution) have, however, allowed direct exploration of the evolution of the chemistry from within the catalyst sample without significant disruption/impact on *operando* conditions.

4. SPATIALLY RESOLVED CHARACTERIZATION TECHNIQUES

Techniques used to spatially resolve the chemical species concentration and temperature distributions throughout a reactor during experimental analysis have been investigated by different groups (*vide infra*). These have focused on obtaining detailed information to understand phenomena occurring on the catalyst surface and in the catalytic reactor under *operando* conditions. These studies have resulted in a growing number of important publications describing the development and application of experimental-based spatially resolved intracatalyst reaction distributions, examples of which are discussed in the subsequent sections. Significantly, these techniques provide the detailed data sets and enable unique opportunities for developing robust catalyst models which can accurately calculate the spatiotemporal reaction evolution throughout the catalyst under realistic operating conditions.

4.1. Electromagnetic Probes for Spatially Resolved Catalyst Characterization. The techniques presented in this section can be classified and defined as "spatial imaging of catalytic reactors." A number of detailed discussions on imaging of spatial heterogeneities within catalytic reactors have been reported,[36−38] and so only a limited selection of key reports are highlighted in this section for a number of analysis techniques. This fast growing field has attracted attention in the past decade and can be divided into three different groups depending on the technique used for analysis: optical spectroscopy, synchrotron-based and magnetic resonance techniques.

Mirodatos et al. have developed a new experimental DRIFTS cell to spatially resolve the surface species on a planar microstructured catalytic reactor (Figure 2). The cell is optically accessible via an infrared (IR) transparent window. *In situ* spatially resolved DRIFTS analysis was obtained by translating the cell under the IR beam, along the full length of the microstructured catalytic reactor.[39] Using this technique, it was possible to obtain a surface map of adsorbed species and gas concentration, and subsequently, to use the information gathered to establish a microkinetic model for the CO oxidation over Pt/Al_2O_3 and $Pt/CeO_2{-}Al_2O_3$. Catalytic plates can be considered to be analogous to a single channel of a catalytic monolith. However, neither single channels of a monolith or catalytic plates are commonly used, and with the emergence of other techniques to study real catalytic monoliths

DOI: 10.1021/acscatal.5b02602
ACS Catal. 2016, 6, 1356−1381

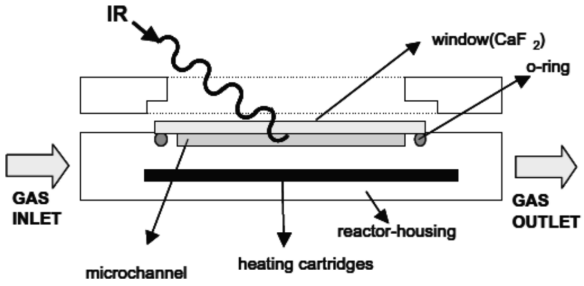

Figure 2. Representation of the optically accessible DRIFTS microstructure reactor. The IR beam is fixed while the reactor is moved to achieve spatially resolved spectra for the length of the catalytic plate. Reprinted with permission from ref 39. Copyright 2010 Elsevier.

operando (*vide infra*), the application of this methodology may be limited.

With a similar approach, Urakawa et al.[40,41] developed a DRIFTS and Raman cell to spatially and temporally resolve the surface species during NO_x storage-reduction (NSR) over a $Pt/Ba/CeO_2$ catalytic plate. This technique is potentially applicable to other spectroscopic techniques, e.g. surface second harmonic generation or UV. The principle is similar to that of Mirodatos et al. as the catalytic plate can be moved using an *x*-*y*-*z* stage. This enabled the study of dynamic surface and bulk processes of NSR via combined space- and time-resolved spectra and gas concentrations. Consequently, improved spectral band assignment was possible and more in depth insights into the surface and bulk processes were reported. As stated previously, however, the use of catalytic plates is not common and so limits the potential application of this technique.

The development of *in situ* XAFS was initiated by Couves et al.[42] (combined with XRD) and further developed by Clausen et al.[43] and followed by other groups.[44−47] Further development by Baiker et al.[48,49] (Figure 3), based on the

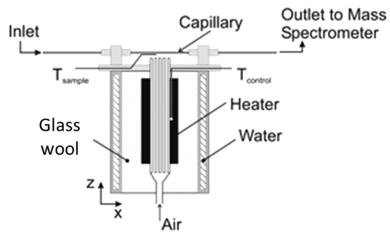

Figure 3. Schematic drawing of the catalytic reactor used for *in situ* spatial resolution under XAFS. The catalyst was loaded between two glass-wool plugs in the capillary. The capillary is heated by a hot gas stream, created by flowing air or N_2 through a heating element. The effluent flow from the capillary was analyzed by mass spectrometer. This assembly (*in situ* cell, heater) was mounted on a translation table to enable the alignment of the sample in the fixed X-ray beam. Reproduced with permission from ref 48. Copyright 2004 PCCP Owner Societies.

techniques developed by others groups,[43−46] led to a catalytic reactor which can be moved during the experiment using an *x*−*y*−*z* stage to obtain *operando* spatially resolved information regarding the catalyst structure. The reactor operates in a flow-over mode using pressed (13 mm diameter by 2 mm thick) catalyst pellets, or flow-through mode using a 1.5 mm capillary filled with catalyst powder. Using this setup, reaction profiles can be resolved along the powder-catalyst bed. Grunwaldt et al. improved this system with the incorporation of a Charge Coupled Device (CCD) camera to allow a full-field X-ray imaging experiment to study the spatial variation in catalyst oxidation state during partial methane oxidation over a Rh/Al_2O_3 catalyst.[50] Consequently, an axial distribution of the Rh-oxidation state across the catalyst bed was mapped in 2D, the first reported instance of XAS monitoring of a catalyst inside a spectroscopic cell.[50]

There have been a number of recent advances in spatially resolved catalyst measurements using synchrotron-based techniques. For instance, Zhang et al.[51] have applied synchrotron X-ray absorption spectroscopy (XAS) to obtain *in situ* spatially resolved profiles of some CO oxidation catalysts, combined with end-pipe MS data. Although the system was designed primarily for powders, it is capable of studying small structured catalysts including pellets and monoliths. A detailed description of the specifications and designs was disclosed, which, although specific to the synchrotron facility used, can be adapted to similar environments. Carbon foils served as X-ray transparent windows which are also chemically inert, temperature resistant, and mechanically robust. In this work, transmission XAS was studied over a Pt/Al_2O_3 catalyst, while Pd/Al_2O_3 and Ag/Al_2O_3 were investigated using XANES in fluorescence mode. It is reported that the system is easy-to-use and relatively inexpensive, making it ideal for maximizing beam-time efficiency via rapid sample changeover since one cell can be used for analysis, while duplicate cells are preloaded with samples in preparation for analysis.

Gänzler et al. were able to apply spatially and time-resolved *operando* XAS, IR thermography, and online MS at the reactor outlet to investigate oscillatory CO oxidation over a Pt/Al_2O_3-based diesel oxidation catalyst.[52] Either *in situ* XAS structural evaluation experiments (carried out using a quartz capillary microreactor) or temperature profile information from IR thermography (conducted with a sapphire capillary microreactor) were simultaneously obtained with MS catalyst activity measurements. The data obtained from the IR/MS experiments were correlated with that of the XAS/MS experiments, essentially providing a spatial and temporal profile of how catalyst temperature, Pt oxidation state, and co-ordination environment of absorber atoms evolved within the catalyst bed, combined with MS activity data. It should be noted that while the IR thermography profiled the entire catalyst bed, no more than four axial points were measured with XAS, and the MS data was from end-of-pipe sampling only. As such, there were no reported spatially resolved MS profiles within the catalyst, nor was there any simultaneous recording of XAS and IR thermography. The data helped to identify a more reactive, reduced-Pt species and a less-reactive oxidized Pt species, the relative proportions of which were controlled by $CO:O_2$ concentration ratio, reaction temperature, and reaction flow rate. It was stated that by using this methodology, the structure−activity relationships could be understood and there were a number of proposed processes which could be studied including (selective) oxidations of hydrocarbons and the treatment of NO_x. This complementary approach of IR thermography, *in situ* XAS, and MS demonstrated the ability to broadly characterize the spatial and temporal CO oxidation oscillations *in situ* and under operating conditions. Previously, a similar report was published by Figueroa and Newton wherein the simultaneous XAS, DRIFTS, and end-pipe sampling MS investigations of CO oscillations over a Rh/Al_2O_3 catalyst were

DOI: 10.1021/acscatal.5b02602
ACS Catal. 2016, 6, 1356−1381

conducted. In this case, the XAS data were reported as a function of catalyst bed depth at six axial points.[53]

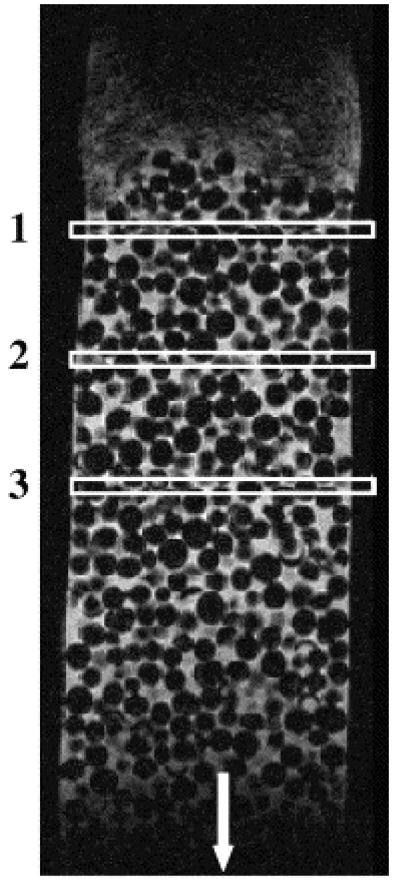

Figure 4. 2D cross sectional image of a ^{1}H 3-D RARE magnetic resonance image of the spatial distribution of liquid within a fixed bed of catalyst particles (black circles). The white rectangle sections correspond to sections from which ^{1}H NMR spectra were reported. The white arrow shows the direction of the supercritical flow of the reactants, whereas the lighter shaded *parts* are the liquid, which changes color due to concentration variations. Reprinted with permission from ref 58. Copyright 2002 Elsevier.

Other notable examples of X-ray techniques in spatially resolved studies includes the comparison of transmission Bragg scattering and synchrotron radiation X-ray diffraction during redox cycling conditions as a function of bed depth (complimented with UV−vis and Raman data);[54] a combination of synchrotron μ-XRD-CT and μ-absorption-CT (CT = computed tomography, thereby allowing spatial distributions of solid phase changes from within a Ni/Al_2O_3 catalyst to be observed in 3D during CO methanation;[55] and high-energy X-ray diffraction (HXRD) imaging to study the spatial and temporal distributions of the structure of a zeolite catalyst for the methanol to olefin process under *operando* conditions.[56] Also of note is the recent development by Pistidda et al.[57] of a system for *in situ* spatially resolved synchrotron radiation powder X-ray diffraction (SR-PXD). This technique was applied to study ammonolysis of metal hydrides. This is a stoichiometric reaction between hydride powders and gas-phase ammonia, and although catalysts were not involved this study, the technique could certainly be easily adapted for the purpose of heterogeneous gas-phase catalysis.

Gladden et al. have significantly contributed to the development NMR for catalyst characterization (Figure 4) by obtaining 1D, 2D, and 3D profiles of the catalytic reactor under experimental conditions.[58−61] Interesting results have been reported and simultaneous composition and temperature profiles within the catalyst bed were obtained under *operando* conditions. However, the sensitivity of the NMR technique limits its use to studies with a liquid phase. Additionally, the nature and the type of atoms that can be followed by the technique are also limited to NMR active nuclei with sufficient concentration and usable spin, and therefore, the majority of systems follow ^{1}H and/or ^{13}C nuclei within the reactor.

Nic an tSaoir et al.[62,63] developed a spatially resolved technique called near-infrared diffused transmittance tomography (NIRDTT) to obtain 2D and 3D temperature and flow composition profiles of water vapor within fluidized and packed bed reactors (Figure 5). This significant advance in tomography has been attributed to advances in high-speed electronics and improved fiber optic technologies. In this system, an NIR laser and a focal planar array (FPA) NIR detector were aligned on opposite sides of the reactor. The laser source and detector

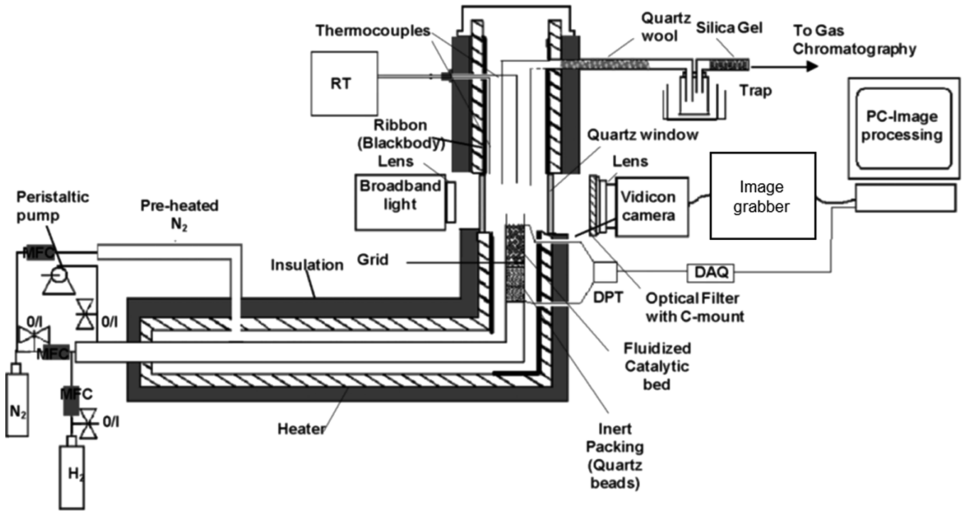

Figure 5. NIRDTT imaging technique for spatial resolution. The camera and detector are mounted on a turn table which rotates around the fixed reactor to provide the spatially resolved profiles via tomographic analysis. Reprinted with permission from ref 62. Copyright 2012 American Chemical Society.

DOI: 10.1021/acscatal.5b02602
ACS Catal. 2016, 6, 1356−1381

were simultaneously rotated (around a vertical axis in Figure 5) to measure the diffused transmission through the bed packing and the transmission through water vapor.

From the results, it was possible to observe nonuniform distributions in both composition and temperature. It is important to note that the use of near-infrared significantly limits the range and concentration of species that can be followed, because of the practically spectrally ubiquitous nature of H_2O absorption transitions and corresponding potential for interference with other species of interest. Greater H_2O-interference-free analytical opportunity may exist in the mid-IR (MIR), which can be utilized for more complex reaction systems such as selective catalytic reduction (SCR).[2] It should be noted that such a study which utilizes spatially resolved mid-IR spectra is still to be reported. Nevertheless, the IR region is excellent for H_2O quantification. It was, however, reported that this technique was suitable for catalytic applications since catalysts for CO oxidation, ozone decomposition, water−gas-shift, and Fischer−Tropsch can be deactivated by water vapor.

Recently, Zellner et al.[64] have applied 2D spatially resolved planar laser-induced fluorescence (PLIF) to determine the absolute NO concentration throughout the reduction of NO using a diesel oxidation catalyst (Pt/Al_2O_3), while exit flows were monitored with IR and MS (Figure 6). Gas-phase

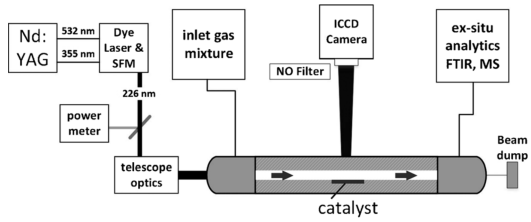

Figure 6. System for 2D spatially resolved PLIF. The combination of translation stage and an observation window above the catalyst sample allowed for the collection of the spatial profiles with the ICCD camera. Reprinted with permission from 64. Copyright 2015 John Wiley and Sons.

fluorescence was induced by a thin laser-light sheet and was observed (in 2D) with an intensified CCD camera. The NO concentration profiles were monitored as a function of both operating temperature (200, 250, and 300 °C) and different residence times. Greater vertical concentration gradients were observed at lower flow rates and higher temperatures, and the relationship between these observations, surface kinetics, and reactant diffusion was discussed. LIF has been further utilized to study mass transfer limitation induced concentration variations inside a reactor, obtaining localized kinetic data, and yielding insights of the catalytically active phase.[65] A similar approach has been utilized to generate axial profiles of LIF and Raman measurements by Mantzaras et al.[66,67]

Titze et al.[68] have recently reported a microimaging IR microscopy approach to obtain gas species profiles during the catalytic hydrogenation of benzene to cyclohexane over a Ni catalyst (Figure 7). Using the specific IR-active molecular vibration absorption fingerprints for benzene and cyclohexane, 2D concentration profiles were determined by recording the spatial dependence of the IR absorbance through the catalyst. The technique was capable of recording the evolution of gas species concentration distributions within the catalyst bed during reaction. Ultimately, reaction rate constants and diffusivities were obtained as well as their Arrhenius dependences. As such, IR microimaging is a useful spatially resolved technique with time-scale temporal resolution in the order of seconds, which can operate at temperatures up to at least 100 °C and potentially higher temperatures. In this instance, however, it would be limited to the use of high concentrations and molecules with high IR sensitivity because the optical path length is very short.

The invasive nature of any measurement is influenced by the nature of both the probe basis and access methodology. In many applications, techniques based on electromagnetic interactions can be effectively noninvasive relative to those based on physical probes. Nevertheless, in some instances, even electromagnetic-based techniques can change the nature of the device under evaluation (e.g., high-energy sintering or volatilizing material), in which case even these can become invasive.[69,70] Monolith-supported catalyst performance can vary from channel to channel, and the performance of a given channel is influenced by its surroundings. In addition, interior channels, which may be readily accessible via small physical probes, may lack direct access for electromagnetic probes. Methodologies to create access for electromagnetic probes can cause even inherently noninvasive techniques to be practically invasive or of limited relevance; that is, the access

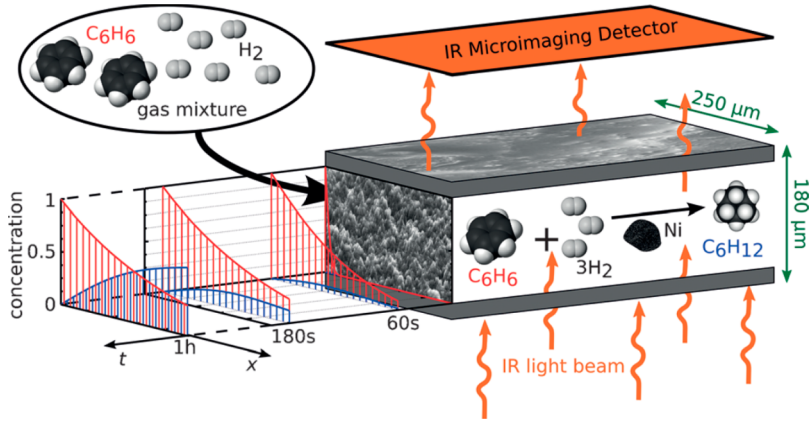

Figure 7. System for microimaging with IR microscopy. An IR light beam is passed through the sample and then the local concentrations of reactants and products are determined from the spatial dependence of the IR attenuation. Reprinted with permission from ref 68. Copyright 2015 John Wiley and Sons.

DOI: 10.1021/acscatal.5b02602
ACS Catal. 2016, 6, 1356−1381

methodology can be invasive. For instance, real-world catalyst reactors do not typically have optical access windows, as shown in Figures 2 and 6, for instance, and the associated temperature- and thermophretic-driven concentration gradients. Moreover, some noninvasive techniques may provide bulk-averaged line-of-sight properties and may not resolve spatial property variations along the line of sight, which might be resolved via physical probes. Additionally, line-of-sight methodologies require at least two points of optical access on opposite sides of the reactor, which many practical (nonspecialized) reactors do not have, and adapting reactors to achieve such extensive optical access can significantly change their nature. To undertake tomography, even more extensive optical access is needed, which requires a very specialized reactor; if the reactor housing (and perhaps the catalyst itself) is transparent to the electromagnetic probe, then the technique can be more broadly applicable to practical reactors. Practically all experimental measurements involve trade-offs, and they are potentially invasive and limited to some degree. While the potential impacts of physical probes (as discussed in the next section) may be easily imaginable, access methodology is often the primary driver of electromagnetic-based techniques and must be considered in a serious or rigorous assessment of invasive nature. As an example, Rasmussen et al.[2] reported a combined surface IR spectra and analyzed gas-phase study (from the same axial point), where holes have been drilled in the monolith walls to improve the IR signal. As such, an analysis of the impact of such holes on flow patterns in the monolith should be undertaken in order to assess the extent of the invasive nature.

4.2. Physical Probes for Spatially Resolved Catalyst Characterization. This section reports on techniques using physical probes located within the catalyst bed to monitor temperatures, including thermocouples and optical fibers for temperature monitoring, and gas concentrations via tubes and capillaries for sample extraction.

In 1985, Baiker et al. developed a nonisothermal, nonadiabatic fixed-bed pilot reactor designed for fast measurement of axial and radial temperature and concentration profiles during dynamic experiments.[71,72] A network of thermocouples and IR analyzer probes were used to measure the temperatures, while GC sampling probes were used to analyze the gas concentrations, at locations throughout the catalyst reactor as indicated in Figure 8. The probes were located at different positions along the catalyst bed with a thermocouple every 10 cm and a GC probe before and after the catalyst bed. The aim of this technique was to assess the degree of complexity necessary for a kinetic model to describe the hydrogenation of toluene using an industrial catalyst in a nonisothermal and nonadiabatic fixed-bed. The experimental data was compared with simulation, and it was reported that a simple one-dimensional model was sufficient to describe the system.

This equipment was one of the first developed to obtain spatial resolution information regarding temperature and species concentrations within a catalyst bed under reaction conditions in order to provide data with which to optimize the kinetics. Interesting data was obtained, but the use of so many IR and/or temperature probes throughout the bed was very invasive, disturbing both the bed and the flow. Furthermore, one can assume that the size of such probes (which were not provided) were significantly larger 30 years ago (when this work was published) compared to those currently available. In addition, this system had limited spatial resolution with respect to the temperature (probe every 10 cm or more).

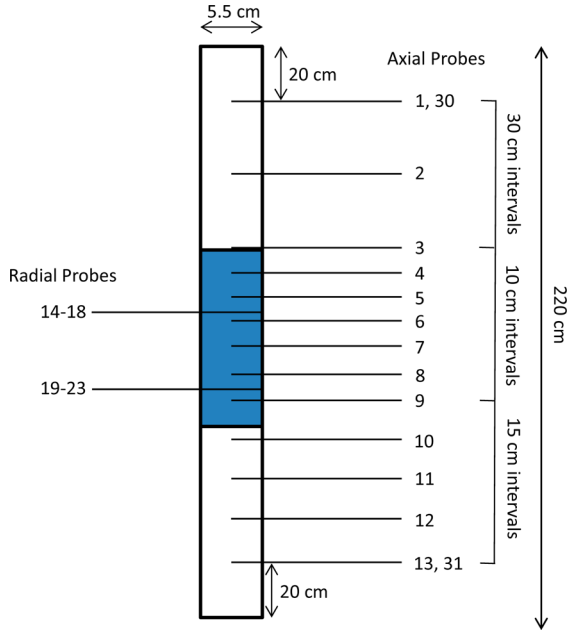

Figure 8. Schematic of catalytic reactor with axial (1−13, 30−31) and radial (14−23) physical probe measuring devices within the catalyst bed (blue) and the inert packing (white). Locations 1 to 23 correspond to the thermocouples and IR-analyzer sampling probes, while 30 and 31 are the GC sampling probes. This drawing is interpreted and adapted with permission from ref 71. Copyright 2009 John Wiley and Sons.

The gas-concentration data obtained with the system did not provide spatial resolution as the GC probes were located before (zero conversion) and after the catalyst bed (maximum conversion), which corresponds to end-pipe sampling. However, with growing recognition of the value of intracatalyst spatio-temporally resolved characterization for advancing detailed catalysis knowledge and research, improvements building on such early studies were realized in terms of spatial and temporal resolution and the minimally invasive nature of physical probes. These improvements leveraged the availability of new and/or improved equipment (increased reliability, reduced sizes and prices), with more accurate and powerful techniques, which have been developed to provide spatially resolved profiles of gas concentrations and temperatures, mainly within structured catalyst beds.

4.2.1. Spaci-MS. In the late 1990s, Partridge et al. at Oak Ridge National Laboratory (ORNL) developed the spatially resolved capillary-inlet mass spectrometer (Spaci-MS) technique in collaboration with Currier et al. at Cummins Inc.[6,7,73] The aim of the technique was to accurately monitor spatio-temporally dynamic automotive catalyst systems; although some applications and development focused on broader research, including engines,[7] fuel cells,[74] and catalytic partial oxidation (CPOx) of methane and propane,[75] the primary focus has been elucidating the network and sequence of reactions within fully formulated and model-formulation automotive catalysts coated on honeycomb (or "channelized") monoliths. The system was configured to be minimally invasive with the use of a very thin (O.D. 150 μm) fused silica capillary which sampled small (ca. 10 μL min^{-1}) quantities to a fast time response mass spectrometer for analysis. With fixed capillary locations, the Spaci-MS approach achieved both quantitative and high temporal response measurements under *operando*

DOI: 10.1021/acscatal.5b02602
ACS Catal. 2016, 6, 1356−1381

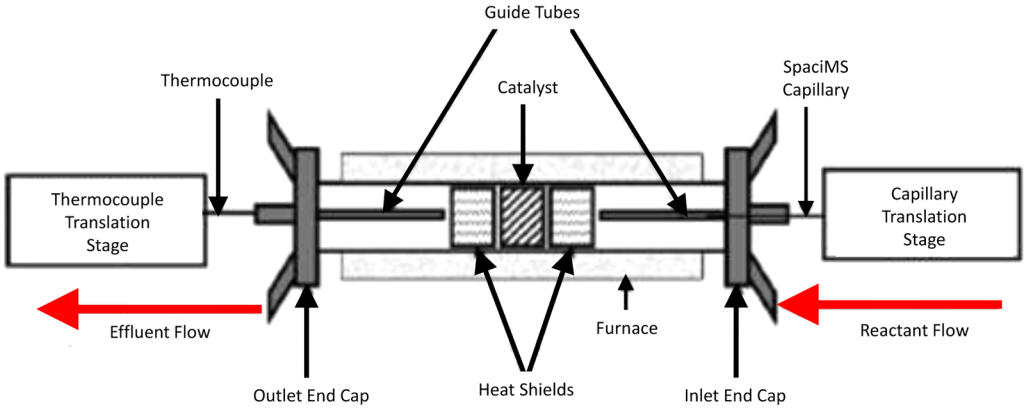

Figure 9. Schematic representation an original Spaci-MS. Reproduced with permission from ref 75. Copyright 2010 The Royal Society of Chemistry.

conditions using real engine exhaust. Moreover, with applications to commercial 300 cell-per-square-inch (cpsi) monolith-supported catalysts, the technique was effectively noninvasive in that the capillary was ca. 2.8% of the channel size and sampled 0.01% of the nominal channel flow rate. The technique was further improved to obtain simultaneous spatially and temporally resolved information.[74,76−82] The improved system allowed movement of the capillary within a monolith channel, which provided for spatial resolution along the full length of the catalyst bed; manual and automated capillary translation was implemented as required for the specific study. For example, very high reaction gradients in a catalyzed partial-oxidation reformer were resolved using 0.3 mm capillary translation steps and a stepper-motor controller. In another example, Figure 9 shows a schematic of two full-size lean NO_x Trap (LNT, NSR, NO_x storage and reduction) catalytic monoliths in the exhaust of a diesel engine and the location of the sampling capillary and the thermocouples, which were used for the first full-scale engine-based Spaci-MS application. In this early study, LNT lean-rich cycling was implemented using in-pipe diesel fuel injection between the engine and catalysts to create the required catalyst transient operation; these systems later evolved to incorporate cylinder-managed reductant generation, eliminating the in-pipe injection.

In broader applications, the Spaci-MS technique was used to quantify species distributions inside the channels of a catalytic monolith used for NO_x storage/reduction (NSR) under cyclic lean and rich conditions.[6,7,73−82] These investigations focused on $Pt/K/Al_2O_3$-based catalysts to study the regeneration of the catalysts at low temperatures and the impact of H_2 and CO on the system. The data obtained with the Spaci-MS provided spatial resolution and simultaneous observation of several reactions depending on the position of the probes in the monolith. The investigations focused on the $Pt/K/Al_2O_3$-based model as well as fully formulated commercial catalysts to elucidate the regeneration chemistry.

For instance, it was found that, in the case of catalyst regeneration by CO at 430 °C, CO oxidation by residual gas-phase O_2 was very efficient, requiring only a small front section of the catalyst; therefore, the downstream NO_x reduction occurred in the absence of gas-phase O_2.[79] The spatiotemporal resolution of reactions further revealed that CO reaction with H_2O (i.e., water−gas shift) becomes significant only where both O_2 and NO_x are almost depleted.[78] Distributed Spaci-MS measurements inside a working catalyst also led to an improved understanding of the intermediate role of NH_3[82] which had been postulated in the literature.[83] The intracatalyst measurement not only confirmed the intermediate NH_3 role but also clarified the temperature dependence of partitioning between direct-H_2 and intermediate-NH_3 pathways in the regeneration of NSR catalysts by H_2. Another practically important chemistry, N_2O formation, was recently addressed by an ORNL and University of Chemistry and Technology Prague team using Spaci-MS.[84−88] In that work, the spatiotemporal distribution of storage and conversion of NO_x, oxidant and reductant species was compared with information regarding the global performance trends (e.g., selectivity) to identify the critical roles of local oxidation state of precious metals in determining local N_2O selectivity.

In yet other work, the effect of sulfur was investigated and was shown to have varying distributed impact on NSR, oxygen storage capacity, and water−gas-shift reaction.[80,81] Such detailed information on the distributed impact of sulfur on different catalyst functions helped to explain unusual integral catalyst performance trends. For instance, it was discovered that a significant increase observed in NH_3 selectivity at the catalyst outlet with progressive sulfation was in fact due to a decreased NH_3 consumption by oxygen storage capacity downstream of the NSR zone; that is, sulfur poisoned the NO_x storage sites along the length in a plug-like manner, thus continually displacing the NSR zone downstream and thereby shortening the downstream OSC-only zone. These examples demonstrate an important and unique contribution of spatially resolved analytics to catalyst research: uncovering chemistry details relevant to practical catalyst systems by understanding spatiotemporal interplay among various catalyst functions and reactions.

The first prototype of Spaci-MS allowed the extraction of information from catalytic monoliths necessary for a better understanding of the phenomena. Further developments were made in collaboration between ORNL and Queen's University Belfast (QUB). The modifications incorporated an automated multiport valve and translation system with a network of corresponding capillaries and thermocouples enabling automated axial and radial mapping of composition and temperature throughout a catalyst monolith. A differential-sampling approach was implemented, in contrast to the direct sampling used in the original ORNL systems, allowing for capillary sampling rate to be tuned (in the μL to mL range) to balance the trade-off between temporal resolution and invasive nature appropriate to the specific experimental investigation. The multivalve port allowed up to 16 capillaries to be used

DOI: 10.1021/acscatal.5b02602
ACS Catal. 2016, 6, 1356−1381

and made it possible to sample gas at several locations in the monolith while thermocouples simultaneously measured temperature profiles (Figure 10). The invasiveness of the sampling

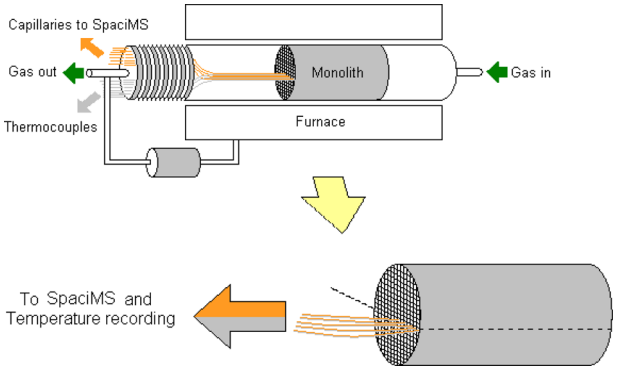

Figure 10. Schematic representation of the Spaci-MS. For the initial scan(s), thermocouples and capillaries are positioned just upstream of the monolith inlet (zero conversion). Then the thermocouples and capillaries are gently pulled using the actuator system, with scans taken at regular axial points to generate 3D spatially resolved temperature and gas-concentration profiles. Reproduced with permission from ref 90. Copyright 2010 The Royal Society of Chemistry.

capillaries within the monolith channel was investigated using computational fluid dynamics (CFD) and showed to have limited effect on the system[89,90] (Section 5). The development of the second generation, fully automated Spaci-MS by QUB and ORNL (in conjunction with Cummins, Hiden Analytical and Y-12 National Security Complex) was awarded an R&D 100 award in 2008, in recognition of it being among the top 100 technologies commercialized that year.[91]

As an evaluation reaction for the new Spaci-MS, CO oxidation was investigated using a commercial honeycomb-monolith oxidation catalyst. The investigation allowed observation of a phenomenon known as kinetic oscillations, which were dependent on the sampling location in the monolith, the feed concentrations and the temperature. Resolution of this spatiotemporally complex catalyst system demonstrated the advanced capability of the new Spaci-MS, and the rich nature of the corresponding data.[89,90] The development of Spaci-MS has brought an original way of obtaining spatially resolved data concerning the gas concentrations and temperatures.

Epling et al.[92] designed an imaging technique for spatially and temporally resolving temperatures within a catalytic monolith. This technique was based on infrared thermography, and therefore, the probe is inherently noninvasive; however, the required optical access has some degree of invasive nature, as discussed in the previous section. The technique measures monolith surface temperature from the intensity of the IR radiation emitted by the monolith using an IR camera. The reaction investigated was NSR over a $Pt/Ba/Al_2O_3$ catalyst. Spatial resolution of the temperature was obtained from which it was possible to deduce the distribution of the NO_x adsorbed species along the length of the catalyst.[92]

The technique of Epling et al. was improved by combining it with Spaci-MS functionalities, which added the spatial resolution of the gas composition from within the monolith.[93−98] Two thermocouples located in the monolith were used to measure the temperature for comparison with the IR thermography. The new system was used to investigate the oxidation of propylene over a Pt/Al_2O_3 monolith.[93−95] The evolution of the gas composition and the temperature within the monolith as a function of time enabled determination of the reaction location within the monolith, the influence of thermal degradation and effect of sulfur exposure. A diesel oxidation catalyst (DOC)[96] was also investigated, and it was demonstrated that H_2 and CO were oxidized first, prior to the other hydrocarbon (HC) species present.

4.2.2. Spaci-IR. While Spaci-MS provides a powerful tool for spatially and temporally resolving gas concentrations inside a catalyst monolith under realistic conditions, the mass spectrometer used for quantifying the gas composition requires careful and time-consuming calibration steps and significant postprocessing of the data sets to ensure accurate speciation of complex gas mixtures with overlapping mass fragments. For example, measuring the concentrations of a mixture containing NH_3, N_2O, NO, NO_2, and N_2 such as might be found inside an operating NH_3 SCR catalyst can be a very difficult and time-consuming process due to the overlapping ion fragments from these species. To avoid the mass spec calibration complications, Epling and co-workers developed a new technique, called Spaci-IR, which uses a Fourier transform infrared (FTIR) spectrometer rather than a mass spectrometer as the primary analytical tool for quantifying the gas composition.[97] This technique is particularly well-suited to the aforementioned NH_3 SCR application, as NH_3, N_2O, NO, and NO_2 all have fairly intense and easily differentiable IR absorption bands.

While calibration and quantification are generally easier with FTIR than with MS, the Spaci-IR approach introduces a different set of challenges. To generate sufficient IR absorption for quantification of gas concentrations, the FTIR gas transmission cell has to operate at near ambient pressures and be large enough to enable a long IR absorption path length. One state-of-the-art FTIR spectrometer optimized for gas analysis (MKS Instruments Multigas 2030) is designed to operate at 1 bar absolute pressure and has an IR path length of 5.1 m through a gas cell with a total volume of 200 cm.[3] While this cell volume is not a problem for typical catalyst effluent measurements, the capillary sampling system used for Spaci measurements limits the amount of gas that can be sent through the FTIR, due to both the small diameter of the sampling capillary and the desire to avoid significant changes in the flow patterns within the catalyst sample. Low flow rates significantly degrade the transient response capabilities of the FTIR and, in extreme cases, can result in steady-state measurement errors due to incomplete gas exchange in the transmission cell. To avoid these issues, Epling and co-workers designed a sampling system that included an N_2 dilution flow to increase the gas flow rate through the FTIR.[97]

The system consisted of a 0.43 mm OD, 0.32 mm ID, 300 mm long fused silica capillary connected to a valve to control the flow of gas sampled from inside the catalyst. The valve was connected to a tee fitting through which the 240 cm^3 min^{-1} N_2 dilution flow was introduced. The catalyst sample was held at slightly elevated pressure (1.05 bar) to drive flow through the sampling capillary, and the outlet valve was adjusted to maintain a capillary flow of 15 cm^3 min^{-1}. This flow rate corresponds to roughly half of the total flow through each catalyst monolith channel. The combination of a larger sampling capillary and higher flow rate increases the probability that the sampling technique will alter the flow distribution through the catalyst, making this implementation of Spaci-IR more invasive than many Spaci-MS setups. The ∼15:1 dilution

DOI: 10.1021/acscatal.5b02602
ACS Catal. 2016, 6, 1356−1381

ratio was quantified by tracking the dilution of the CO_2 concentration, which passed through the catalyst unreacted. While this setup allowed enough flow through the FTIR to ensure sufficient gas exchange, the 0.8 min turnover time precluded transient measurements. Also, the dilution flow reduced the concentration of species measured in the FTIR, decreasing the sensitivity of the instrument and increasing measurement uncertainty. While a state-of-the-art FTIR may have a nominal accuracy of ±1 ppm for most species, the 15:1 dilution ratio translates to an accuracy of ±15 ppm of the species measured inside the catalyst, which represents significant uncertainty under high conversion conditions. Nevertheless, Epling and co-workers successfully deployed their Spaci-IR system to measure concentrations of NH_3, NO, NO_2, and N_2O inside a Fe exchanged beta zeolite monolith core sample.[97] By translating the capillary under steady-state conditions, they mapped concentration as a function of catalyst position under a wide range of temperatures and feed gas compositions. They showed the effects of temperature and inlet NO_2/NO_x ratio on the distribution of SCR reactions along the catalyst length, and they used these measurements to draw several conclusions regarding the kinetics of the SCR reactions on the Fe-exchanged zeolite: (1) NO oxidation is the rate-limiting step for NO SCR; (2) NH_3 inhibits the NO SCR reaction; and (3) the relative rates of the three potential SCR pathways decrease in the order fast (NO + NO_2) SCR > NO_2 SCR > NO SCR.[97] Luo et al. later used the same apparatus in an investigation of C_3H_6 poisoning of NH_3 SCR over a Cu-exchanged beta zeolite monolith core sample.[98]

Huo et al. used a slightly modified Spaci-IR setup to measure spatial distributions of NH_3 storage on a commercial Cu chabazite SCR catalyst after exposure to NH_3 pulses of varying concentration and duration.[99] Their setup utilized a significantly larger sampling capillary (0.68 mm OD, 0.53 mm ID) and a higher operating pressure (1.26−1.30 bar) than the previous studies to drive a much higher sample flow rate (44 cm^3 min^{-1}) through the capillary. Interestingly, these authors intentionally withdrew a higher flow rate through the sampled channel than the average flow through the unsampled channels. They estimated the GHSV through the sampled channel as 60 000 h^{-1}, while the overall GHSV based on the total flow through the entire catalyst volume was 30 000 h^{-1}. Such a high flow rate through the sampled channel would result in flow maldistribution through the remaining catalyst channels. However, the authors make the point that they are only sampling the gas from upstream of the capillary in the channel they are analyzing, so what is happening downstream of the capillary or in adjacent channels should not impact their measurements. This argument relies on the assumption that gas cannot pass through the substrate wall, which is likely not true for the common cordierite-based substrates which are porous in nature. Regardless, this particular approach is substantially more invasive than most other Spaci techniques. In spite of the sampling approach, the work by Huo and co-workers is interesting in that it represents the first attempt to use Spaci-IR to measure spatially resolved surface inventories rather than just local gas concentrations. They show how the NH_3 storage distribution is impacted by the inlet NH_3 concentration, the catalyst temperature, and the duration of the NH_3 pulse. They also show how NH_3 redistributes along the catalyst through desorption and readsorption on downstream storage sites.

Song and co-workers also utilized a Spaci-IR system to measure spatial distributions in a Cu-exchanged small-pore zeolite SCR catalyst.[100] To improve response time in the FTIR, these investigators used two sampling capillaries (0.68 mm OD, 0.53 mm ID) positioned in adjacent catalyst-monolith channels, and a slightly elevated reactor pressure (1.1 bar) to generate a higher net sample flow (80 cm^3 min^{-1}). They also operated the catalyst at a higher GHSV (60 000 h^{-1}) than was used in prior studies to have a higher gas flow through each catalyst monolith channel from which to sample (100 cm^3 min^{-1}). The higher capillary flow allowed the authors to decrease the dilution ratio to 10:1, thereby increasing FTIR accuracy at low concentrations, while simultaneously improving the transient response of the measurements due to the higher overall flow to the transmission gas cell. While the flow through each capillary was less than half the nominal flow through the individual gas channels, the authors saw evidence of higher than anticipated flow through the sampled channels based on comparisons between NH_3 storage capacity measured through Spaci-IR and calculated from traditional catalyst effluent measurements. This observation illustrates the significant challenges in designing a minimally invasive Spaci-IR sampling system that enables accurate measurements under transient conditions. In retrospect, perhaps a better approach would be to operate the capillaries in an isokinetic sampling regime, in which the fraction of gas removed from the catalyst channel is equal to the fraction of channel area blocked by the capillary. To account for the apparent discrepancies in sample channel flows, the authors used a corrected GHSV (69 000 h^{-1}) in all of their calculations and analysis.

In spite of these challenges, Song et al. were able to use their Spaci-IR system, combined with carefully designed transient experimental protocols, to measure spatially resolved gas concentrations and surface NH_3 inventories under steady-state SCR operating conditions at multiple temperatures for inlet NO_2/NO_x of 0 ("standard" SCR) and 0.5 ("fast" SCR).[100] These spatially resolved data sets were then used to calibrate the kinetic parameters for a model based on a detailed global reaction mechanism with two distinct active sites. This work demonstrates the substantial advantages afforded by Spaci data sets in model calibration and validation.

To clarify, despite the convenience of FTIR, it is indeed possible to measure NH_3 at ppm-levels in the presence of H_2O and N_2 at percent level using MS. Heeb et al.[101] used CI-MS to measure NH_3 variations in gasoline-engine exhaust, and Chatterjee et al.[102] used CI-MS to measure NO, NO_2, and NH_3 variations in diesel exhaust. In separate studies, Epling[103] and Olsson[104] have monitored NH_3 at ppm levels via EI-MS by using separate ionizer settings for the NH_3 and other-species measurements; Epling made measurements in the presence of H_2O and N_2 at percent levels, and Olsson in the presence of percent-level H_2O. This takes advantage of the varying ionization potential of the various species; for example, N_2, H_2O, O_2, NH_3, and NO have ionization potentials of ca. 15.6, 12.6, 12.1, 10.1, 9.3 eV, respectively.[105] In their experiments, Olsson used a Hiden MS and was able to actively vary the ionization potential as the quadrupole mass filter stepped through the various scanned m/z values, whereas Epling used a Pfeiffer MS and performed separate experiments with fixed ionization potential for monitoring the various species. There can be temporal resolution benefits to using a fixed ionization source, as every instrument change involves an associated settling time; however, active potential switching may improve experimental efficiency. Nevertheless, these works demonstrate the ability to monitor ppm-NH_3 levels in the presence of H_2O

DOI: 10.1021/acscatal.5b02602
ACS Catal. 2016, 6, 1356−1381

Figure 11. Picture of the system of Vogel et al. The gas sampling capillary is positioned above the catalytic plate. The capillary is then moved along the length of the catalytic plate to obtain the spatially resolved concentration profiles. Reprinted with permission from ref 107. Copyright 2010 Elsevier.

and N_2 at percent levels using MS, and the studies exhibit methods for addressing the specific experimental priorities and trade-offs at hand.

4.2.3. Techniques Similar to Spaci-MS and Spaci-IR. Vogel et al.[106,107] developed a technique to obtain spatially resolved gas composition measurements in an optically accessible catalytic plate reactor, which was intended to replicate the conditions within a single monolith channel; a picture of the system is reported in Figure 11. The spatial resolution of the gas composition was achieved via a moveable sampling capillary located above a catalytic plate with the capillary effluent analyzed using GC and MS. The catalyst surface temperature was determined simultaneously using an infrared camera viewing the catalyst through a quartz glass window. Methanation and water−gas-shift reactions over a commercial Ni- based catalyst under different temperatures and pressures were investigated therein. The spatially resolved gas composition and the temperature measurements along the catalyst plate were used for kinetic studies.[106,107] In addition, a full CFD study was conducted to investigate the phenomena above the catalytic plate including contact time with the catalytic plate and the impact of the sampling probe, as is discussed in Section 5.

Similar to this approach is the stagnation flow reactor (SFR)[108] where species concentration profiles are obtained using a quartz microprobe which is connected to an FTIR and MS. In the study reported, this microprobe was in close contact with the surface of an Rh/Al_2O_3-coated catalytic plate. Kinetic measurements of CO oxidation for varying $CO:O_2$ ratios were made with the catalyst temperature at 251, 400, and 600 °C. The experimental results were compared to numerical simulations (see Section 6 for more details). In all cases, it was not possible to achieve total CO conversion, although larger concentration gradients were observed at higher temperatures due to increased conversions.

Behm and co-workers[109,110] have developed a new technique called scanning mass spectrometry (SMS), which is able to measure the gas composition above catalytically active microstructures or arrays of these microstructures with a lateral resolution of better than 0.1 mm under reaction conditions. The technique allows quantitative determination of the reaction rates on individual microstructures. A 3D representation of the scanning mass spectrometer is shown in Figure 12. The reactions

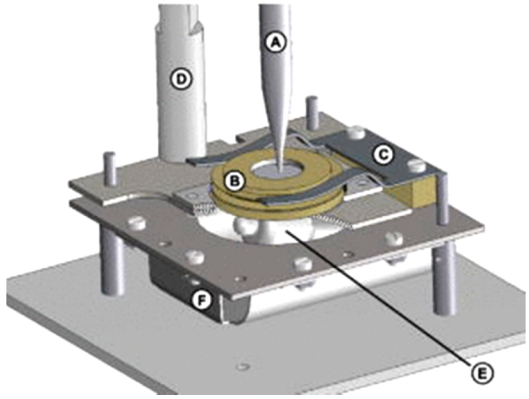

Figure 12. Three-dimensional representation of the scanning mass spectrometer. (A) is the sample stage with the capillary, (B) is the sample holder, (C) is the clamp mechanism, (D) is the distance sensor, (E) is the halogen bulb for heating, and (F) is a tantalum shielding. Reprinted with permission from ref 110. Copyright 2007 AIP Publishing LLC.

are carried out in a reaction chamber containing the catalyst under study. A separate analysis chamber containing the mass spectrometer is mounted on top of the reaction chamber. A capillary tip is positioned very close to the catalyst surface to probe the local gas composition within the reaction chamber. The catalyst is supported on a three-axis translation stage with a very high lateral and vertical precision to allow analysis of the entire catalyst surface. The sampled gases were analyzed by a quadrupole mass spectrometer.

Recently, Chorkendorff and co-workers[111] extended the use of the scanning mass spectrometer to vacuum conditions, which enabled use of ultrahigh vacuum techniques for controlled *in situ* preparation and surface characterization of catalysts. The technique is very similar to that reported by Behm et al., with the major difference being that the sampling and the gas delivery are made via the same probe. However, both investigation methodologies did not quite correspond to the common arrangement of these type of catalysts (i.e., plug flow reactor), and the relevance of the information obtained to *operando* conditions remains to be demonstrated.

4.2.4. Foam Monolith Spaci-Like Techniques. In addition to the broad automotive-catalyst applications, Spaci-type

DOI: 10.1021/acscatal.5b02602
ACS Catal. 2016, 6, 1356−1381

measurements have been applied to study reforming and oxidation catalysts. A Spaci-MS study of methane oxidation using various oxygen concentrations over a $Pt/Pd/Al_2O_3$ catalytic monolith has also recently been reported by Bugosh et al.[112] The results have indicated that complete methane oxidation can occur in both lean and rich conditions. Under rich conditions, an oxidative zone is located near the reactor inlet, while a mixed partial oxidation/reforming zone is present downstream. There was also evidence of a transition between these two clearly defined zones. These results yielded some mechanistic insight given that partial oxidation of methane still occurs under methane rich conditions, indicating that lattice oxygen is involved. From experiments that co-fed CO and methane, it was apparent that CO oxidation occurred first, depleting the gaseous oxygen concentration, thereby promoting direct partial oxidation of methane further downstream, for which it is speculated that lattice oxygen which diffuses to the catalyst surface is responsible.

Recently, Hettel et al. have also used a capillary sampling technique to obtain spatially resolved concentration profiles from within a Rh-coated monolith for the CPOx of methane.[113] In the same study, the invasive nature of the capillary and a comparison to a kinetic model were made, and these aspects are further discussed in Sections 5 and 6, respectively. Similar work has also been published elsewhere.[108] Gas compositions at a number of axial points were monitored with FTIR and MS, while the gas-phase temperature was monitored with a thermocouple and the surface temperature monitored by an optical fiber connected to an IR pyrometer. As such, both temperature and concentration profiles were generated for the CPOx of methane reaction at 290 °C. Consequently, it was possible to identify two separate reaction zones for total oxidation/reforming (at inlet, 0−1 mm) and reforming reactions only (1−11 mm). The latter reaction zone was enabled by the initial-zone exotherm, and reforming reactions were promoted due to oxygen-deficient conditions resulting from O_2 consumption in the total oxidation process. The reaction sequences and general findings are similar to those reported earlier by Partridge et al.[75]

The same technique[113] was utilized by the same group[114] to further investigate the CPOx of methane using a Pd/Al_2O_3-coated monolith upstream of a Rh/Al_2O_3-coated monolith, which was compared to both Pd/Al_2O_3 only and Rh/Al_2O_3 only systems. The important findings from this work were that, despite a higher surface temperature exotherm, Pd was less effective for the reforming reactions. It was also reported that there were differences in the mechanisms for the formation of syngas over the two metals. For Pd, syngas formation did not occur until the oxygen had been depleted, meaning CPOx in this instance occurred by an indirect route. However, due to the high catalytic activity of Rh for CPOx of methane under these conditions, it was not possible to exclude a role of direct partial oxidation to syngas.

This technique has also been used to study diesel oxidation catalysis using model lean exhaust gas.[115] After catalyst aging, CO light-offs were monitored at 235 °C. The results of the catalytic activity were correlated to catalytic surface area. It was reported that, as expected, both surface area and activity decrease with catalyst aging, and higher aging temperatures increased this rate of catalyst deactivation. The concentration profiles obtained were also compared to a kinetic model (see Section 6 for more details).

A Spaci-like approach to obtaining gas concentration and temperature profiles from a fixed catalyst bed has also been developed, first by Schmidt et al. at the University of Minnesota, and then by Horn et al. at the Fritz-Haber Institute.[116−130] This technique was originally used to study drilled foam catalysts, initially with an open ended capillary, but evolved to incorporate a capped-end-capillary with a side wall sampling orifice (see Figure 13). The technique was also used to

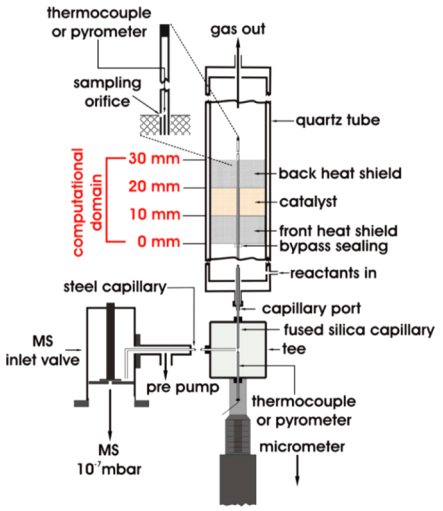

Figure 13. Schematic representation of the system for resolving species and temperature distributions within a foam-monolith catalyst showing the location of the different elements of the system. Reprinted with permission from ref 118. Copyright 2008 Elsevier.

investigate the mechanism of the CPOx of methane over Rh- and Pt-coated over Li/MgO on α-Al_2O_3 foam support, as well as oxidative dehydrogenation of ethane to ethylene over a molybdenum oxide catalyst supported on a bed of γ-Alumina spheres. The experimental data were combined with kinetic simulations for CPOx of methane studies and allowed a better understanding of the reaction mechanisms prevailing.[117−119] The influence of the sampling on the reaction kinetics was not discussed.

The principle of the technique is similar to that of the Spaci-MS, since a single movable axially mounted capillary is used to sample the gases. The main difference is that a large-bore (700 μm OD, 520 μm ID) capped-end sampling capillary with an orifice (O.D. 0.3 mm) drilled in the side wall is used to sample the gases, instead of an open ended capillary for the Spaci-MS. The capillary is inserted in a hole drilled through the foam monolith; the drilled hole is barely larger than the capillary OD to allow capillary translation while minimizing gas bypassing through the open annular region. The capillary wall orifice is located at an appropriate distance from the capped end such that the capillary fills the accommodating foam-monolith hole for the full range of capillary translations. Other differences with the Spaci-MS include incorporating a thermocouple within the sampling capillary to measure gas temperature. Spatial resolution of gas concentration and temperature is obtained by moving the probes along the axial position in the drilled channel within the catalyst foam.

Recent improvements of the technique have been made by Horn et al. The new reactor design allows for measurements to be collected at temperatures up to 1300 °C and pressures up to 45 bar.[125−127] The sampling system of the technique was

DOI: 10.1021/acscatal.5b02602
ACS Catal. 2016, 6, 1356−1381

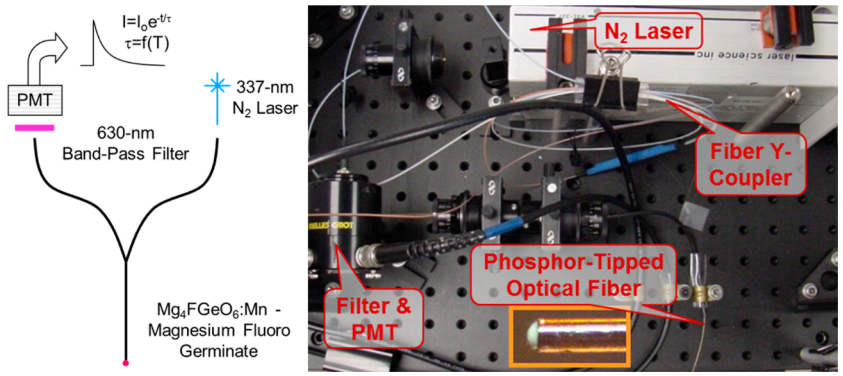

Figure 14. Schematic and picture of optical-fiber-based phosphor thermography instrument, applied to measure transient temperature distributions within operating honeycomb-monolith supported catalysts.

further developed to allow for capillary rotation, which provides an improved spatial resolution of the catalyst bed.

The most recent development of this system is the collection of spectroscopic data regarding the catalyst surface.[116,127] This is accomplished through insertion of a Raman optical fiber probe into the sample capillary instead of the thermocouple.[116,127] In this application, the Raman-probe tip is aligned with the capillary sampling orifice so that the gas-composition and surface-spectroscopic characterization are from the same spatial region of the catalyst bed; however, the Raman is averaged over a 360° perimeter region of the sample capillary while the orifice samples from a point on the perimeter.

Schmidt, Horn, and co-workers have very significantly contributed to the development of spatially resolved techniques for characterizing catalyst supported on foam monoliths and bead beds; in the bead-bed applications, the support-bead OD (1 mm) was similar to that of the sampling capillary (0.70 mm). In these applications, the sampling probe was not considered to be invasive due to the strong radial mixing in foam-monolith and bead-bed catalysts (i.e., vis-à-vis channelized honeycomb monolith applications where a sampling capillary might change the flow profile).[131] This system is limited to catalytic foams and large pellets, although it could be applied to investigate monoliths, and like Spaci-MS and Spaci-IR, it is not well-suited to powder-catalyst applications; specifically, the sampling probe size is much greater than the typical powder catalyst particle size and as such would be far too invasive for accurate analysis.

4.2.5. Techniques for Temperature Distribution. Donazzi et al.[132−138] developed a technique for spatially resolved surface temperature measurements within structured (monoliths and drilled foams) catalysts. The technique is based on the use of a side-looking optical fiber connected to a pyrometer for measuring wall temperature distributions within a honeycomb catalyst; measurements resolution is dictated by the local fiber-channel geometry and numerical aperture of the fiber, and distributions are resolved via fiber translation. The application of intracatalyst optical fiber physical probes was presented as noninvasive for honeycomb-monolith applications, which is true for a broad range of applications as discussed later; in general, optical fibers have the same physical invasiveness considerations of a capillary, but without the sampling flow considerations. The technique does not resolve gas-composition profiles within the honeycomb monolith, although effluent gas analysis was performed using gas chromatography. The CPOx of methane to syngas over a Rh-based catalyst with different catalyst loadings and the influence of channel size was investigated.[132−135] The temperature profiles were used to develop a kinetic model for the reaction.[136]

Choi et al.[79] have described the application of phosphor thermography for resolving spatiotemporal transient temperature distributions within an operating honeycomb-monolith-supported LNT catalyst. Phosphor thermography is based on the temperature-dependent excited-state lifetime of a phosphor transducing material, and the technique is typically implemented by optically exciting a phosphor and analyzing the resulting phosphorescence.[139,140] Measurements can be made via direct lifetime detection using pulsed excitation, or via phase-sensitive detection with modulated excitation. A range of phosphors exist which are active in various temperature bands and have varying lifetimes; these can be selected to meet the temperature and time requirements of a specific experiment. Partridge et al. have adapted this technique to honeycomb-monolith-supported catalyst applications by applying a thin phosphor coating to the tip of a working optical fiber,[79] as shown in Figure 14 (previously unreported). The technique is similar to Spaci-MS in that small (ca. 200-μm OD) optical fibers are used, measurements are made at the phosphor tip, and distributions are resolved by translating the optical fiber. In general the sensitivity and temporal response are tuned via phosphor specification/selection and thickness of the phosphor layer, respectively. Because the working phosphor-tipped optical fiber has very low thermal conductivity, it will not significantly spatially broaden temperature gradients as would measurements from a conductive temperature probe; thus optical-fiber based phosphor thermography can more accurately resolve high temperature gradients compared to even fine-wire thermocouples.

Optical-fiber techniques have the ability to directly resolve temperature distributions along their length, in contrast to the method of spatially scanning a single-point sensor, via methods employing fiber Bragg gratings (FBG)[141] and optical frequency domain reflectometry (OFDR).[142,143] The techniques are based on spectral analysis of backscattered light from various points along the optical fiber length. Multipoint distributed measurements can be made by writing FBGs into the fiber at the desired measurement locations, each of which provides return signals for analysis. Continuously distributed measurements are available from OFDR as the scattering signal originates from natural variations along the fiber length; thus, return signals are generated throughout the fiber length in a unique fingerprint-like pattern. In both cases thermal expansion changes the location between the scattering sites, inducing spectral changes in the backscattered light which is calibrated to determine

DOI: 10.1021/acscatal.5b02602
ACS Catal. 2016, 6, 1356−1381

temperature; since fiber strain can cause equivalent displacements and confound the measurements, pure temperature measurements require strain-free fiber conditions.

Nguyen et al.[144] have applied a commercial OFDR (OBR 4600, Luna Innovations) to measure temperature distributions along a 7.5 cm long monolith-supported catalyst resulting from NH_3 oxidation; distributions were measured with 3 mm spatial resolution and 0.9 Hz (1.1 s) temporal resolution. The application used a horizontal catalyst reactor, with the measurement fiber resting in a relatively strain-free orientation along the lower wall of the probed channel. Greater strain-induced noise was observed at the fiber free end and higher space velocities due to flow-induced fiber movement. Nevertheless, the technique has great potential for transient distributed temperature studies, as was further demonstrated in subsequent work.[145]

4.2.6. Spaci-FB for Powder Catalyst Bed Applications. Most of the techniques for spatial resolution within catalytic reactors described above have been designed to investigate structured catalysts (pellets, monoliths, foams) or "model" catalysts (catalytic plates). In fact, despite being the most commonly utilized textural form for catalysts in research at the lab scale, until recently, there has been no technique designed to noninvasively investigate reaction distribution within a packed powdered catalyst bed.

In recent studies, Touitou et al. reported the development of a spatially resolved technique for powdered catalyst beds (later named as Spaci-FB for fixed bed) and results obtained through proof of concept/validation.[146−148] Initially, a prototype system with a manual linear transfer mechanism (Figure 15)

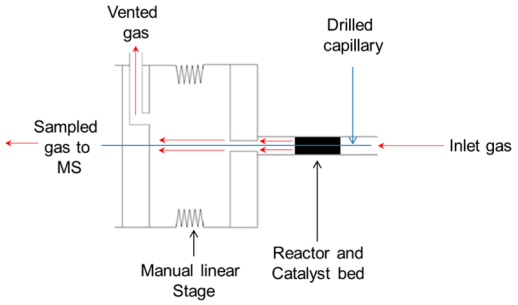

Figure 15. Representation of Spaci-FB prototype.[146] The capillary in this case was fixed, and the linear stage translates the reactor/packed bed across the sampling holes, thereby providing the spatially resolved gas concentrations.

was developed which acted as a proof of concept of the spatial resolution technique for packed powdered catalyst beds.[146]

A description of the individual components and the modifications of these up to and including the assembly of the completed prototype was disclosed.[146] The technique was designed to have negligible impact on the packed powdered catalyst bed with the use of some of the smallest equipment commercially available. The key element in this case was the closed-end sampling capillary (75 μm ID, 150 μm OD), which had three sets of gas sampling holes (3 pairs of sampling holes of 20 μm diameter, each set having 180° orientation, and located within a sampling zone 0.5 mm in length) drilled on the capillary side using laser ablation. The size of these sampling holes was small enough to prevent catalyst particles from entering the probe and causing blockages. A number of validation tests of the prototype Spaci-FB technique were conducted, where gas-concentration profiles of CO oxidation over 1 wt % Pd/Al_2O_3 were measured to demonstrate the technique and its sensitivity to different experimental conditions (i.e., temperature and feed). Effects of both temperature and the presence of H_2 in the gas mixture were studied and the promotion of the reaction by both temperature and hydrogen was reported.

Based on the positive results obtained with the Spaci-FB prototype, further technique development and improvements were implemented;[148] these included improved control and precision with an automated transfer mechanism, an improved heating system, and the capability to simultaneously record temperature and gas concentration (Figure 16). The gas

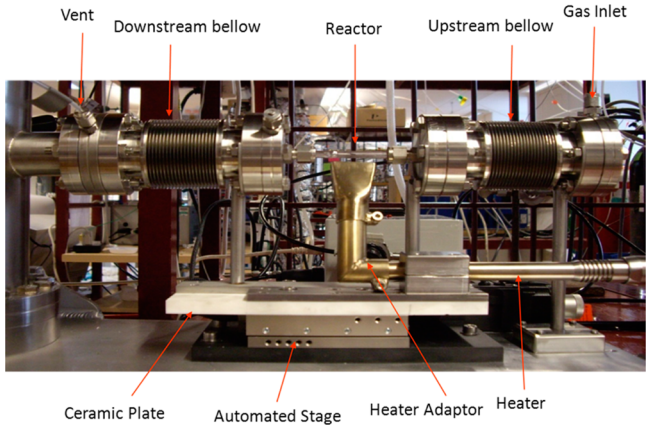

Figure 16. Automated Spaci-FB system. The capillary is fixed and the automated stage translates the bellow system/reactor, passing the packed bed across the sampling holes, thereby providing the spatially resolved gas concentrations. A thermocouple is positioned inside the gas sampling capillary, thereby providing simultaneous spatially resolved temperature profiles. Reproduced with permission from ref 148. Copyright 2013 The Royal Society of Chemistry.

sampling holes of the capillary were also machined in a less-destructive manner using a xenon focused ion beam, but the dimensions and locations of holes remained consistent. In order to address the capability for temperature recording, a thermocouple with the smallest outer diameter commercially available (80 μm) was inserted inside the capillary, and aligned with the gas sampling orifices. The catalyst bed was housed in a quartz tube and heated with a novel hot air blower heating device, which enabled *operando* optical access to the catalyst with a view to future coupling with spectroscopic techniques.

Further validation tests were conducted which studied the effect of temperature and reactant concentration on the gas and temperature profiles. The results of these validation tests highlighted the impact of the improvements which enabled the gas-concentration and temperature profiles to be determined with twice the spatial resolution (every 0.5 mm) of the prototype system. The precise movement of the automated stage allows for even higher spatial resolution, but the limiting factor in this instance is the length of the sampling zone itself (i.e., 0.5 mm). Consequently, conversion light-off and the temperature exotherm were both profiled accurately with a high spatial resolution.

The capabilities of the Spaci-FB have also been assessed in terms of performance and influence of the probe on the measurements[149] (see Section 5 for more details). A previously

DOI: 10.1021/acscatal.5b02602
ACS Catal. 2016, 6, 1356−1381

reported microkinetic model[33] has been refined to accommodate the Spaci-FB probe and comparisons made with experimental results for CO oxidation under different conditions has also been reported,[149] and more details are discussed in Section 6.

4.3. Summary of Spatially Resolved Characterization Techniques. The emergence of spatially resolved techniques has allowed the opportunity to study a range of catalytic textural forms, systems, and sample environments, thereby providing intracatalyst analytical profiles of structures, gas concentrations, and/or temperature. While using techniques which employ intracatalyst physical probes, it is necessary to conduct an evaluation of the invasive nature of these probes under the operating conditions.[113] Examples of evaluations of this kind are reported in Section 5. In most cases, the use of physical probes has been reported to be minimally invasive (*vide infra*). Consequently, reliable insights of kinetics and surface processes which were previously unavailable are now accessible. Such detailed data can be used to improve kinetic models by bridging the "knowledge gap" between traditional catalyst analysis and theories/models,[113] as is discussed in further detail in Section 6.

5. ASSESSING THE INVASIVE NATURE OF PHYSICAL SAMPLING PROBES

As already stated in this work, spatially resolved techniques enable fundamental and applied studies of catalysts in their most realistic conditions. A major advantage of these techniques is the ability to conduct experiments under *operando* conditions using real catalysts (either structured or powdered), as opposed to using "model" catalysts (and/or using conditions to suit the analytical method). Moreover, because the incremental steps of the intracatalyst conversion profiles are resolved, these techniques can enable kinetic studies under actual operating (temperature, space velocity, etc.) conditions rather than those necessary to achieve differential conditions across the entire catalyst. These characteristics are a major advancement in the understanding of catalysts under true operating conditions, and this significance should not be underestimated.

An important aspect to consider using intracatalyst physical probes for spatially resolved measurements is the impact these probes may have on the system (i.e., how invasive are the probes). This has to be assessed using, for example, numerical or experimental analysis, and there is still some debate as to how invasive the probes can be.[112]

5.1. Numerical Methods for Assessing Invasive Nature. Numerical analysis (using computational fluid dynamics (CFD)) has been applied to assess the invasiveness of probes by Bosco and Vogel[106] using 2D and 3D fluid dynamic modeling under different conditions to study the velocity field within a replicated monolith channel, as applied to the recording of spatially resolved gas-concentration and temperature profiles. In this study, the Navier−Stokes equations were solved for a pure nitrogen flow. The inlet velocity was 0.14 m s^{-1} and the selected Reynold's numbers for the system were far from critical limits and so the existence of a Laminar flow was well justified. There was little flow in the *y*-direction (channel cross section) and the velocity profile was consistent throughout the reactor channel. It was noted, however, that a Laminar flow did not initially materialize, but rather the fluid had swirling (eddies) structures caused by the monolith obstruction. Consequently, the catalyst was removed from the initial 15% of the channel so that the catalysis was studied under purely Laminar flow (without eddies) conditions. Consequently, it was possible to demonstrate that the probes used were minimally invasive.

A similar CFD assessment was conducted by Sá et al.[90] for their Spaci-MS application to study spatiotemporal distributed intracatalyst CO oxidation oscillations. This numerical analysis was conducted using a 3D model of fluid flow and mass transfer within catalytic monolith channels, and comparisons were made between cases with and without a probe capillary in the channels. The boundary conditions described in Sá et al. were average inlet velocity, temperature, gas concentrations, and outlet pressure (atmospheric), measured sampling-capillary suction rate, as well as the Reynolds number. The use of an identical 200 mL min^{-1} volume flux at the entrance of all channels was justified by the laminar flow profile upstream of the monolith (premonolith section) with a maximum velocity at the center of reactor tube (ID 25 mm) housing the catalyst monolith of 0.016 m s^{-1}. Since a 400 cpsi monolith was used, the monolith sample contained 19 channels along the tube diameter. Hence, it was reported that a section of 3 × 3 adjacent channels will receive approximately similar volumetric flow rate. This is not necessarily the case for nonadjacent channels.[150]

It was reported that the cross sectional area of the capillary probes were 4.9% of the channel and that there was negligible invasiveness in terms of flow and mass transfer under the conditions investigated. It was advised that similar evaluations be conducted for applications using higher values of space velocities because the degree of probe invasiveness would be greater at higher space velocity (SV) values and different for each set of operating conditions. In general, the various catalyst, reactor conditions, and probe characteristics have an interrelated impact on the invasive nature of intracatalyst spatially resolved measurements; these characteristics include monolith density (cpsi), SV, probe diameter, and sampling rate. Smaller probe diameter and sampling rates become increasingly necessary at higher monolith densities and SV values to achieve minimally or practically noninvasive intracatalyst measurements. Such practically noninvasive probe conditions can be satisfied for a wide range of catalyst studies enabling spatially resolved intracatalyst measurements and the corresponding critical insights.

The findings of Sá et al.[90] have recently been challenged by Deutschmann and co-workers[113] who claimed that the probes are bound to be much more invasive than previously reported. The rationale for this was based on a claim that the boundary conditions had not been properly described by Sá et al.,[90] and their independent numerical analysis,[113] which was, however, conducted at much higher flow rates/space velocities than that used by Sá et al.[90] Hence, the direct comparison[150] between the numerical analysis conducted by Sá et al.[90] and that by Hettel et al.[113] is debatable.[150]

When critically analyzing such numerical analysis, one should also be mindful of the conditions that have actually been reported. In the case of Hettel et al.,[113] a worst-case scenario has been reported in order to assess the probe invasiveness. This is a sensible and logical approach since one wants to assess the maximum possible impact of the presence of the probes. However, on closer examination, the selected scenarios must correspond to practical configurations. In this case, the capillary was placed centrally in a channel; however, given the horizontal orientation of the monolith and considering the physical nature (flexible rather than rigid) as well as length of the capillary used

DOI: 10.1021/acscatal.5b02602
ACS Catal. 2016, 6, 1356−1381

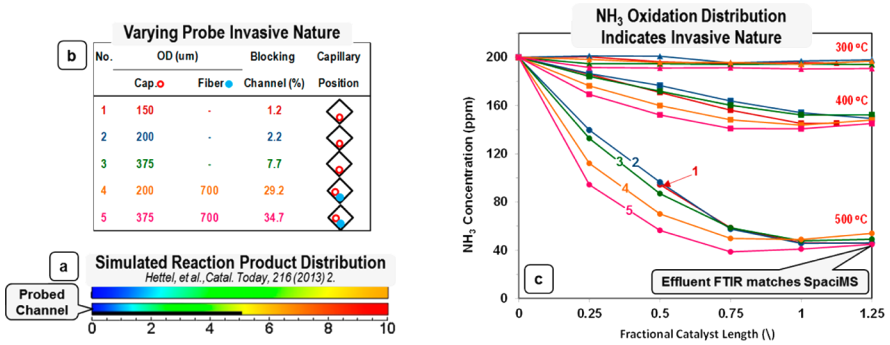

Figure 17. [152] (a) Numerical simulation showing the impacts of an invasively probed catalyst channel. An invasively probed (lower) and unprobed (upper) catalyst channel are shown, with the invasive probe indicated by the black bar lying along the bottom of the lower channel. Flow is from left to right, and bright colors (orange and red) indicate greater conversion. The numerical scale below the channels indicates spatial length in mm; (b) Summary of five intracatalyst probe configurations blocking ca. 1 to 35% of the catalyst channel and spatial orientation of the probes within the probed channel; (c) Spatially distributed NH_3 concentration due to oxidation over a commercial SCR catalyst at three temperatures and the five intracatalyst probe configurations. Panel (a) is reprinted with permission from ref 113. Copyright 2013 Elsevier.

within Spaci-MS, the capillary will not be in the channel center due to gravity. Hence, the worst-case-scenario conditions selected by Hettel et al.[113] are unrealistic, and the cases with the capillary centered on the bottom wall or in the corner on the bottom wall are more realistic configurations. It is important to note that for these latter configurations, Hettel et al.[113] report significantly reduced impact of the probe.[150] This demonstrates the need to carefully consider the actual conditions when comparing intracatalyst measurement techniques. Even individual techniques such as Spaci-MS may be implemented in different ways for various studies; e.g., direct vs differential sampling (impacts capillary sampling rate), vertical vs horizontal reactor orientations, and different capillary diameters, catalyst-monolith densities, and reactor flow rates. As discussed earlier, these experimental parameters have an interrelated impact on the invasive nature of intracatalyst probe measurements, and parameter values that may be practically noninvasive in one combination may be more or less invasive in conditions with different parameter combinations. Thus, similar considerations as used for designing noninvasive methods should be applied to comparing and assessing intracatalyst probe results.

More recently, CFD numerical analysis has been conducted to assess the invasiveness of a probe capillary positioned within a powdered catalyst packed bed reactor.[149] Variations of the flow dynamics in terms of pressure drops and gas velocity along the reactor were investigated for two configurations, specifically with and without a capillary probe. This packed bed was positioned in a reactor tube of 2.50 mm ID and included 3000 spherical particles of 0.25 mm diameter size with the catalyst bed length being 8.00 mm. Due to the additional capillary volume, the bed length increased to 8.50 mm when the probe was inserted in the center of the packed bed. In order to compare with previously reported experimental results,[146,148] the following conditions were applied: inlet velocity of 0.1178 m s^{-1} (Reynolds number less than 30: laminar flow), gas density of 0.6 kg m^{-3}, viscosity of 0.00001 Pa.s, and temperature of 200 °C. From the CFD, the pressure drop was reported to be negligible, 114 Pa without capillary and 124 Pa with the capillary (total pressure 2 bar abs). As such, the pressure drop in both cases was calculated to be <0.1% of the system total pressure. The cross-sectional area of the capillary was 0.7% that of the reactor and hence the exit velocity increased by 0.7%. This was found to be independent of the location of the probe. This variation in exit velocity was sufficiently small to be considered negligible, indicating that the presence of the probes was minimally invasive.

5.2. Experimental Methods for Assessing Invasive Nature. Purely experimentally based methods are available for assessing the invasive nature of intracatalyst probes, in addition to the numerical-based procedures discussed above; although these have been broadly discussed and presented by Partridge et al.,[151] they have not been published heretofore. If an intracatalyst probe is invasive due to its physical size, in applications to open-channel honeycomb-monolith-supported catalysts, it will lower the space velocity in the invasively probed catalyst channel compared to that in the surrounding unprobed channels. The impact of such invasive probing has been simulated by Hettel et al.,[113] as shown in Figure 17a; specifically, an invasive probe will result in higher conversion gradients and possibly higher integral conversion compared to the unprobed channels.[152]

Variations in integral conversion between invasively probed and unprobed channels as shown in Figure 17a creates a step in the conversion profile at the catalyst exit due to mixing of products from the corresponding channels. Specifically, the measured conversion distribution for the invasively probed channel in Figure 17a would show a step to lower conversion at the channel exit (10 mm) and beyond; in most applications, there are many more surrounding unprobed channels, so the conversion step can be significant. Evidence of such experimentally observable signatures of probe invasive impacts can be measured to assess the practical invasive nature of a particular experimental configuration.

Figure 17b,c describe experiments that were performed to assess the invasive nature of various intracatalyst measurement probe configurations and to demonstrate experimental-based methodologies for assessing the same. The experiments were based on NH_3 oxidation over a commercial Cu/SAPO-34 SCR catalyst supported on a 300 cpsi open-channel honeycomb monolith and oriented so that a probe capillary would lie in the channel corner. A 21-channel, 2.45 cm long catalyst core was evaluated at 300, 400, and 500 °C using a gas mixture of 200 ppm of NH_3, 10% O_2, 5% H_2O and Ar balance at 30 000 h^{-1} SV. Spaci-MS was used to resolve NH_3-concentration distributions along the central catalyst channel. Capillaries of various OD (150, 200, and 375 μm) were used to occlude different fractions (ca. 1 to 8%) of the probed catalyst channel cross-sectional

DOI: 10.1021/acscatal.5b02602
ACS Catal. 2016, 6, 1356−1381

area; as all capillaries had the same (75 μm) ID, the capillary sampling rate was the same (ca. 10 μL min^{-1}) for all probing configurations. To investigate the impact of even greater channel blocking, the two larger OD capillaries were used in conjunction with a 700 μm OD optical fiber; in these configurations, the optical fiber extended through the entire probed channel, as the capillary was translated to resolve evolution of the NH_3-oxidation reaction. Figure 17b summarizes the five intracatalyst probe configurations for blocking ca. 1−35% of the catalyst channel and spatial orientation of the probes within the probed channel.

Figure 17c shows the NH_3 concentration distributions through the catalyst at 300, 400, and 500 °C for the 15 (three temperatures and five sampling configurations) separate NH_3 oxidation experiments based on Spaci-MS measurements at the inlet, 25%, 50%, 75%, 100%, and 125% of the total catalyst length (L). The 100% L sample was taken just before the exit of the probed-channel exit. There is negligible NH_3 oxidation at 300 °C (verified by an FTIR gas analyzer at the reactor outlet). Significant NH_3 oxidation exists at 400 and 500 °C, as well as variations in the NH_3 concentration distributions for the various intracatalyst sampling configurations. Specifically, a greater bow (midbed difference) is observed in the conversion distributions for configurations 4 and 5, which block ca. 29 and 35% of the channel area, relative to the less invasive probe configurations; these bows are indicative of higher intracatalyst conversion gradients as discussed above, and they are experimental evidence that the probe configuration is invasive. The 375 μm OD capillary, configuration 3, shows a very slight bow at 500 °C. In contrast, there is no practical difference in the measured NH_3 distributions for the 150 and 200 μm OD capillaries, indicating that these intracatalyst sampling configurations have reached the practical noninvasive limit. In practice, Spaci-MS capillaries of <200 μm OD are typically used for catalyst research, and these measurements indicate this configuration to be practically noninvasive.

To demonstrate how an exit-plane conversion step could indicate invasive sampling conditions, it is useful to consider an alternate experiment where the catalyst was half length (i.e., a case where the 50% L location in Figure 17c is the exit plane). In this alternate case at 500 °C, the effluent NH_3 concentration from both the unprobed and noninvasively probed channels would be ca. 100 ppm, based on the performance of the practically noninvasive configurations 1 and 2; thus, since all catalyst channels would have the same conversion, the combined effluent concentration would be 100 ppm beyond the exit, and there would be no exit-plan conversion step for the noninvasive sampling configurations. In the same alternate case at 500 °C, the invasive configuration 5 would experience a step in the NH_3 concentration across the exit plane from ca. 60 ppm to ca. 98 ppm (i.e., ca. 60 ppm effluent from the probed channel diluted by ca. 100 ppm from the 20 unprobed channels). Of course, these alternate conditions could be generated by doubling the experimental space velocity. Exit-plane conversion steps can be easily implemented and provide a clear experimental measure of the invasive nature of a specific sampling condition.

Figure 17c shows that an exit-plane conversion step may not always be a reliable indicator of invasive nature; furthermore, such conversion steps can be obscured by potential back-mixing dilution if insufficient spatial resolution exists near the catalyst exit. Specifically, although the noninvasive configurations 1 and 2 show the expected flat distributions beyond the exit plane, a conversion step is not clearly apparent for the invasive configurations 4 and 5. It appears that the through optical fiber used in configurations 4 and 5 caused greater back-mixing dilution at the 100% L sampling location, and the anomalous negative conversion trends in the last quarter-catalyst length; clearly, the conversion should continue in the last catalyst quarter consistent with the upstream distributions, and additional sampling could resolve this distribution and the transition to back-mixing dilution; indeed, a conversion step would be more apparent with such additional spatial sampling. The slightly invasive configuration 3 at 500 °C shows a case where invasive sampling may not produce an exit-plane conversion step. For this case, despite the greater conversion at 50% L for the probed channel compared to the unprobed channels (as indicated by noninvasive configurations 1 and 2), all the catalyst channels have reached the same conversion by 75% L. These examples show that although exit-plane conversion steps can indicate invasive sampling, their absence does not necessarily indicate noninvasive sampling. Care should be taken to account for potential back-mixing dilution near the exit, by increasing spatial sampling density in this region. In addition, higher space-velocity experiments, as discussed in the preceding paragraph, are recommended, particularly to detect slightly invasive conditions where the invasively probed and unprobed channels reach similar conversion levels within the catalyst.

If an invasive intracatalyst probe configuration is implemented, there will be a distributed impact along the catalyst length, which will generally be greatest in the inlet region. This is apparent from any of the invasive configurations (4 and 5) in Figure 17c. For example, the enhanced conversion at 500 °C associated with the impact of configuration 4, which blocks ca. 29% of the channel area, is ca. 47%, 25%, and 6% at 25%, 50%, and 75% L, respectively, relative to the practically noninvasive configuration 2 (200 μm OD capillary). In addition to demonstrating the distributed impact of invasive probe configurations, this demonstrates how in worst-case locations using grossly invasive configurations order-of-50% errors can be induced as has been broadly claimed by Hettel et al.[113] (i.e., using probes that block 29% of the channel area, at the channel front where impact is maximized, and for high temperatures where impact sensitivity is greater). However, this grossly invasive claim is not generally indicative of real world intracatalyst sampling methodologies. In general, practically noninvasive intracatalyst sampling configurations can be designed for a wide range of applications and quantified as such via experimental measures, as demonstrated by Figure 17.

5.3. Dimensionless-Parameter Maps for Assessing Invasive Nature. Recognizing the interrelated impact of reactor, catalyst monolith, and probe parameters on the measurement invasive nature, Harold et al. have developed a methodology for quantifying the invasive nature of various parameter combinations.[153,154] The analysis is based on development of dimensionless factors relating the various parameters, for example, capillary diameter and monolith-channel density, sampling flow rate, and probed-channel space velocity. These factors can be plotted over a range of parameter values to generate an invasive-nature map, with regions specifically identified as clearly invasive and other regions as practically noninvasive; the two regions are divided by a boundary where a delta-Z parameter is essentially zero. In applications, proposed experimental parameter combinations are mapped via the dimensionless factors to the invasive-nature

DOI: 10.1021/acscatal.5b02602
ACS Catal. 2016, 6, 1356−1381

space; the parameters can be varied to balance the experimental objectives. Using this method, they plotted configuration C from Hettel et al.[113] (i.e., with the sampling capillary positioned on the catalyst-channel floor) on the invasive-nature map, and they found that it fell in the moderately invasive region; these results are generally consistent with those of the comparison work, which also indicated a capillary situated in the channel corner would be less than half as invasive as the analyzed configuration. On the basis of this, we expect the corner-situated capillary to be practically noninvasive, similar to the experimental analysis presented above. This new dimensionless-parameter mapping methodology represents a significant advancement for enabling design of minimally invasive analysis for intracatalyst measurements.

5.4. Summary of Assessing Invasive Nature of Physical Sampling Probes. The ability of recent advances in intracatalyst spatially resolved sampling techniques to offer previously unavailable insights in terms of surface processes, network and sequence of reactions, and kinetics within the sample is undeniable.[112,150,155] These can provide critical insights including an understanding of the general nature of catalyst reactions, including the following: quantifying the sensitivity of various catalyst functions to aging, and reversible and irreversible poisoning; determining kinetic parameters under the most realistic catalyst structure and conditions; and designing, tuning and validating numerical models of the catalyst process. However, the experimental techniques must be carefully designed such that the physical probes are practically noninvasive and do not change the nature of the catalyst environment being studied; this section has described numerical, experimental and dimensionless-parameter methodologies for designing such noninvasive spatially resolved intracatalyst measurement systems. Even if not completely noninvasive, spatially resolved intracatalyst analysis can provide valuable insights for advancing mechanistic understandings, developing advanced models and optimizing catalyst performance (e.g., including reaction network and sequence, identification of intermediate species, and nature of reaction trends with operation-parameter changes). Ultimately, the veracity of invasive nature claims will depend on the ability of any subsequently derived kinetic model to withstand critical scrutiny (Section 6).

6. ADVANCED SIMULATIONS AND MODELS ENABLED BY SPATIALLY RESOLVED ANALYSIS

Over the past decades, an alternative to laboratory based experiments has been actively pursued to obtain understanding of catalytic processes through the development of kinetic models based on computer calculations.[156] Kinetic models provide improved understanding of phenomena occurring on the catalyst surface but have the advantage of enabling faster and lower-cost development compared to laboratory experiments.[157] The common criticism concerning kinetic models is the question of their accuracy with respect to the phenomena occurring within the catalyst beds and their applicability beyond the conditions under which they were specifically developed and validated. This is a consequence of a lack of comparison between experimental and simulated results, primarily resulting from the difficulty of obtaining measurement data within the reactor during the experiment, that is, due to the lack of techniques available.

Simulations and models can be improved by bridging the "knowledge gap" between traditional catalyst effluent analysis and theories via the application of spatially resolved techniques. This type of study can provide spatiotemporal insights into the complexity of processes and enhance the constraints imposed on the mechanistic models assessed, thereby improving simulation accuracy and fundamental understandings.[136]

A clear value of using spatially resolved reactor data is the ability to determine kinetic parameters of a catalyst model under actual operating conditions. For instance, Matera et al.[65] used LIF data for multiscale modeling based on first-principles microkinetic models to better understand the catalytically active Pd phases for CO oxidation, with the metallic state reported to be responsible for the activity.

With the help of Spaci-MS data, Auvray et al. developed a kinetic model of a Cu-zeolite NH_3−SCR catalyst which was capable of capturing the spatial distribution of NO oxidation, NH_3 oxidation, and SCR reaction over a 200−400 °C temperature range.[158,159] A similar benefit to model tuning and validation was demonstrated by Shwan et al. where LNT modeling work showed that information on the axial NO_x distribution and intermediate NH_3 role is important to accurately predict the outlet NH_3 slip from a $Pt/Ba/Al_2O_3$-coated monolith LNT catalyst.[84] As mentioned earlier, another area where spatial resolution of reactions can significantly enable kinetic modeling is the elucidation of reaction mechanisms resulting from complex spatial interplay among a variety of reaction transients. A good example is an LNT model enhancement achieved via a collaborative research between the University of Chemistry and Technology Prague (UCTP) and Oak Ridge National Laboratory.[85−88,160,161] In this work, the UCTP and ORNL team used Spaci-MS to determine the spatiotemporal distribution of storage and conversion of NO_x, oxygen and reductant species over fully formulated commercial LNTs. By comparing the storage and conversion data with local selectivity values—which were also spatially and temporally resolved—mechanisms underlying N_2O formation were clarified.[85,87,88] In particular, the local oxidation state of precious metal sites was identified as having a critical role in formation of both primary and secondary N_2O peaks observed at lean-to-rich and rich-to-lean transitions, respectively. Residual NO_x and reductant species left on the catalyst surface were the source of the secondary N_2O formation when the gas composition changed to a net lean condition. The learned mechanistic details were incorporated into a global model with reasonable agreement between simulations and experiments with respect to the newly added N_2O chemistry steps.[86,160] In addition to the model enhancement, the chemistry insights obtained from the Spaci-MS investigation led the team to devise a novel LNT operating strategy which minimizes secondary N_2O formation by inserting a short near stoichiometric pulse between lean and rich phases.[161] The stoichiometric gas environment allowed residual NO_x and reductant species to continue to react over fully reduced PGM sites with a high NH_3 selectivity. Importantly, similar model calibrations/validations have been possible for SCR processes using the Spaci-IR technique,[100] demonstrating that spectroscopy can make such contributions in addition to concentration and temperature profiles. As a result of data obtained by Spaci-IR,[100] a one site SCR model was found to inadequately predict both the axially resolved species concentrations and the NH_3 storage distributions. Therefore, the introduction of a second NH_3 storage site, with a capacity based on the difference between experimental and simulated NH_3 concentrations, was able to correct the model resulting in good agreement between observed and

DOI: 10.1021/acscatal.5b02602
ACS Catal. 2016, 6, 1356−1381

simulated species concentration results, as well as the NH_3 storage distributions along the axial length of the monolith.

Spatially resolved data combined with modeling have allowed accessing crucial information unavailable using standard end-pipe approaches. For instance, the degree of complexity necessary for a kinetic model to describe the hydrogenation of toluene using an industrial catalyst in a nonisothermal and nonadiabatic fixed-bed reactor has been assessed in details.[71,72] The reaction had been studied previously at steady state and with deactivation of the catalyst. The experimental data was compared with simulation and it was reported that a simple one-dimensional model was sufficient to describe the system.

A kinetic model for the partial oxidation of light hydrocarbons over a honeycomb monolith catalyst has been developed using experimentally obtained temperature profiles.[136] A previously reported[162,163] dynamic one-dimensional heterogeneous model for a fixed bed reactor was used. This model accounted for balances of mass, energy and momentum for gas and solid phases, including axial convection and diffusion, solid conduction and gas−solid transport terms.[136] The model also included a previously reported thermodynamically consistent single site C1 microkinetic scheme for the production of syngas from methane over Rh which consisted of 82 surface reactions and 13 adspecies.[162,164] It was reported that this model was accurately able to predict both concentration and temperature (both solid and gas phase) spatial profiles for two different catalyst loadings, although there are some variations (Figure 18). These variations were attributed to the pore diameters used (better fits with smaller pores) as well as to variations in heat and mass transfer rates. It was also reported that some further refinements were needed as there may have been some bias in surface temperature recording outside of the catalyst zone due to the methods used (i.e., an optical pyrometer).

Methane partial oxidation inside a foam-monolith-supported catalyst has also been modeled using a pseudo 2D heterogeneous reactor model in CFD simulations.[130] A number of assumptions related to gases and boundary conditions were detailed and equations for conservation of mass, momentum, and energy were all derived from a simplified Navier−Stokes system. Microkinetic models were based on those of Deutschmann et al.[165,166] and Vlachos et al.[167,168] Model profiles for oxygen were found to fit the experimental results reasonably well, but the model profiles for products did not have as good a correlation with the corresponding experimental data (Figure 19).[130] The explanations for this were that one of the microkinetic models under predicts conversion of methane, while the other under predicted the rates of water−gas-shift reactions. Additionally, the surface coverages derived by both microkinetic models did not match with each other, therefore further refinements were needed. Similar work using CFD has been reported for partial oxidation of methane[108,113,169,170] and diesel oxidation reactions[115] inside honeycomb monolith catalysts.

Vogel and co-workers also developed a kinetic model[107] to numerically analyze a channel plate reactor system[106] used for hydrocarbon reforming, such as the methanation of CO. A Langmuir−Hinshelwood expression was used in a 1D reactor model to estimate kinetic parameters, which generated simulated profiles that correlated well with experimental data. A 2D model was also used, which agreed with the results from the 1D model and so it was reported that the 1D was sufficient

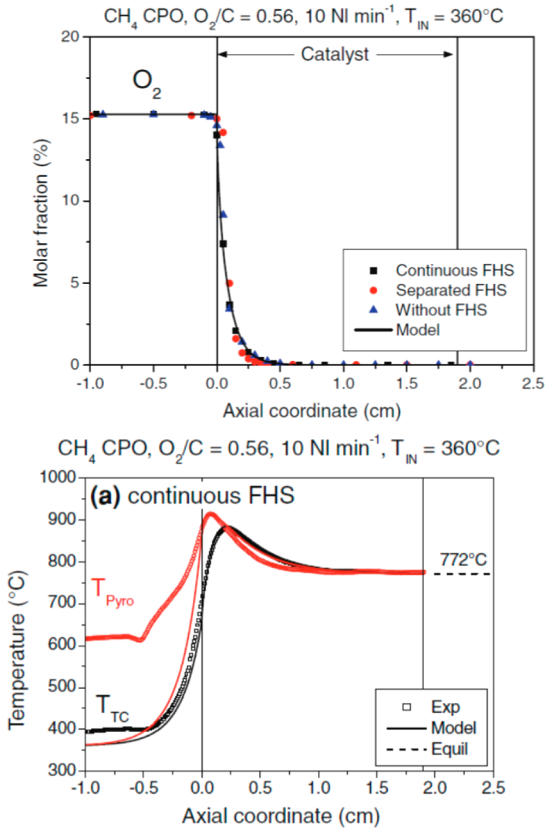

Figure 18. Comparison of experimental and simulated concentration and temperature profiles from the catalytic partial oxidation of methane. Reproduced with permission from ref 136. Copyright 2011 Springer Science and Business Media.

to numerically analyze the plate reactor under the studied conditions. The authors have noted that more experiments (e.g., transients) and increased range of operating conditions (e.g., higher pressure) would allow for a much more thorough assessment of the models.

Wehinger et al. have used 3D governing equations and fluid dynamics simulations to model dry reforming of methane[171,172] and oxidative coupling of methane,[171] using previously obtained axial temperature profiles. For dry reforming of methane only the surface processes (adsorption, surface reaction, and desorption) were described,[171] using a stagnation-flow reactor configuration. It was found that a 1D model could fit the stagnation flow experimental data reasonably well, and so, it was reported that this configuration was well suited to investigate kinetics whenever there is minimal fluidic effects.

Meanwhile, the kinetics for oxidative coupling of methane was based on the reaction rates of the entire system; thus, a porous-media model and 10-step reaction mechanism was utilized for CFD.[171] It was reported that the model was not able to properly simulate the oxidative coupling of methane due to its exothermic nature. In this case, the reactivity was underpredicted, and the model could not generate temperature profiles to match the experimental data. The authors consequently stated that, in the case of highly exothermic or endothermic processes, the studies need to be conducted in well-defined configurations and that experimental spatially resolved concentration and temperature profiles should be utilized for kinetic analysis. This is precisely what these authors reported in further work.[172]

DOI: 10.1021/acscatal.5b02602
ACS Catal. 2016, 6, 1356−1381

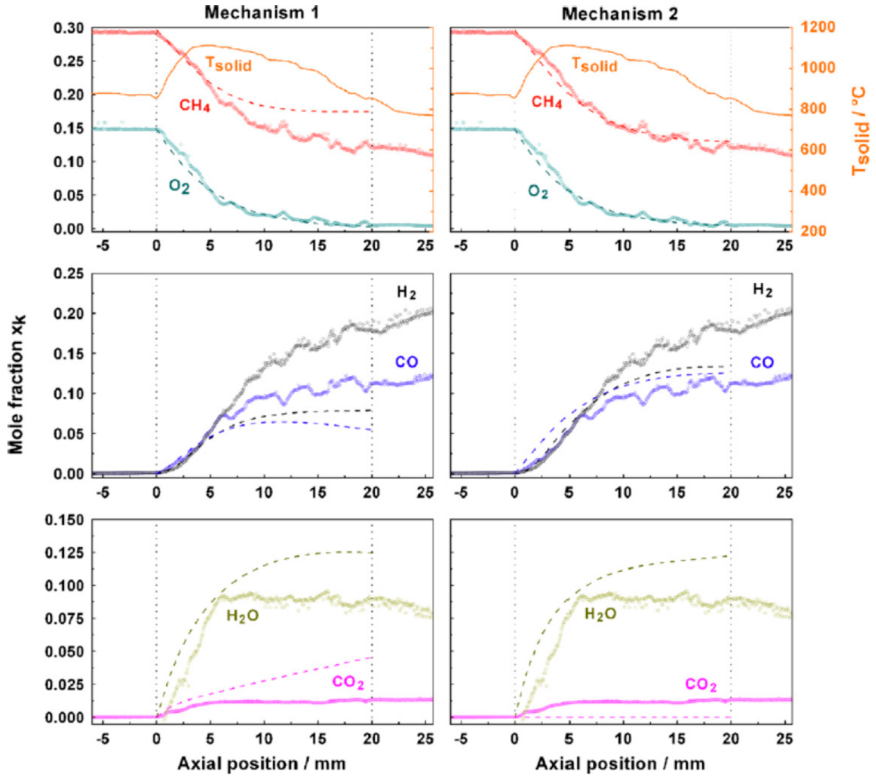

Figure 19. Comparison of experimental and simulated gas-concentration profiles for the partial oxidation of methane. Reprinted with permission from ref 130. Copyright 2013 Elsevier.

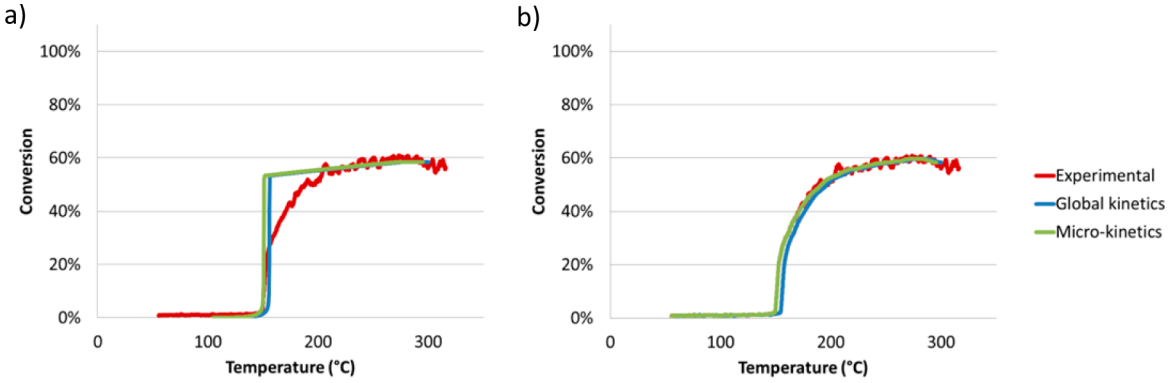

Figure 20. Comparison of experimental and simulated (from global and micro kinetic models) conversion profiles during light-off experiments (a) before and (b) after optimization of mass transfer parameters. Reproduced with permission from ref 34. Copyright 2014 SAE International.

A kinetic model combining a global Langmuir−Hinshelwood methodology (the Voltz method[173]) and a microkinetic approach[32,33] (which included the rates of adsorption, desorption, surface processes, and diffusion) has been reported for the Spaci-MS system for catalytic monoliths.[34,174] The global kinetics approach of this kinetic model runs 18 surface reactions. The microkinetic approach of the model can be utilized provided that the kinetic parameters for the adsorption, desorption, and surface reactions are available. This model was validated for CO oxidation (with varying CO:O_2 ratios)[174] and for the WGS[34] over Pt catalytic monoliths and simulations were compared with experimental results. Data was reported for three axial points representing the start, middle, and end of the monolith (2 mm, 14 mm and 26 mm, respectively). The kinetic model was very accurate for predicting the profiles for the middle and end sections. The simulations for conversion as a function of temperature at the start section were not as accurate, and this identified problems with the mass transfer parameters, which were refined to improve the accuracy of the model (Figure 20).[34] Although not reported in the original work, it is possible that this is a similar phenomenon of the creation of eddies at the front end of the monolith due to the "obstruction" caused by the presence of the catalyst, as discussed previously.[106] The refinement of the mass transfer parameters resulted in a good correlation between the experimental and simulated conversion as a function of axial position profiles (Figure 21).[34] Interestingly, from the CO oxidation it was reported that the microkinetic approach was more effective than the global kinetic approach for predicting the profiles of the processes investigated.[174] From the WGS study, both the global and microkinetic models were found to accurately describe the gas-concentration/conversion profiles.[34]

DOI: 10.1021/acscatal.5b02602
ACS Catal. 2016, 6, 1356−1381

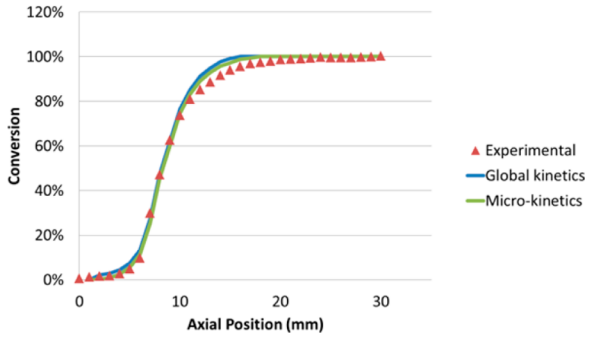

Figure 21. Comparison of experimental and simulated (from global and micro kinetic models) conversion profiles as a function of axial position. Reproduced with permission from ref 34. Copyright 2014 SAE International.

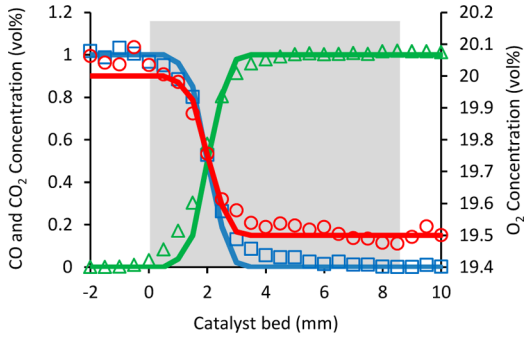

Figure 23. Comparison of experimental (symbols) and semiempirical simulated (solid lines) results of gas-concentration profiles (CO in blue, O_2 in red, and CO_2 in green) from within a packed powder catalyst bed. Reprinted with permission from ref 149. Copyright 2014 Elsevier.

The previously mentioned kinetic model for Spaci-MS[34,174] has been refined for the Spaci-FB system.[149] Both the packed bed and the reactor are modeled in the kinetic study.[149] Information on the catalyst (particles size, volume, surface area, precious metal loading, and precious metal dispersion) as well as physical dimensions such as diameter and length (for both reactor and catalyst bed) and the reactant gas (flow and concentration) were used to mathematically represent the catalyst bed. The reactor was modeled in terms of heat and mass transfer in axial and radial directions. A fully simulated (concentration and temperature profiles) study and a semiempirical (simulated concentrations, experimental temperature) study were reported. Assessing the results with a reported critical error method, it was found that the semiempirical model was better able to predict experimental results of the gas concentration. The heat transfer parameters for the fully simulated model were found to be inadequate as the simulated temperature profiles did not match the experimentally observed results, and this enhanced the errors on the simulated gas-concentration profiles (Figure 22).[149] The semiempirical model uses the experimentally obtained temperature profile, and consequently, a greater accuracy in the simulated gas-concentration profiles was obtained (Figure 23).[149]

By incorporating the findings of the semiempirical model, it will aid the further development of a new fully simulated model to provide a better understanding of catalysts, thereby assisting catalytic development, while also validating the importance of microkinetic models. This was and still remains the ultimate aim of the development of spatially resolved techniques.

This section has shown a broad range of applications where spatially resolved measurements (including spectroscopy, gas concentrations, and temperature profiles) have been used to broadly enable advances in catalyst knowledge and modeling, including determination of kinetic parameters, assessing the validity of conceptual mechanistic pathways and specific models, and insights into practical catalyst operation methodologies for improving performance (e.g., reducing N_2O emissions). In essence there is almost a cyclical and mutual benefit to this where kinetic models can greatly help with the development of catalysts, while experimental results can greatly help with the development of more accurate kinetic models. In this way, spatially resolved intracatalyst measurements play a critical role in enabling the most advanced, accurate, and broadly applicable catalyst models.

7. PERSPECTIVE ON THE FUTURE OF SPATIALLY RESOLVED TECHNIQUES

With the desire to develop and optimize ever better catalysts and catalytic processes has come the quest to develop techniques which are capable of providing more accurate data, desirably under *operando* conditions. Over the past 30 years and more, this has led to the creation, advancement and further evolution of techniques which are now defined as providing spatial resolution, where it is possible to obtain intracatalyst analysis.

Predominantly, however, these *operando* techniques tend to use only one characterization method (such as MS, GC, IR, or XAS) at a time, which means that in order to observe

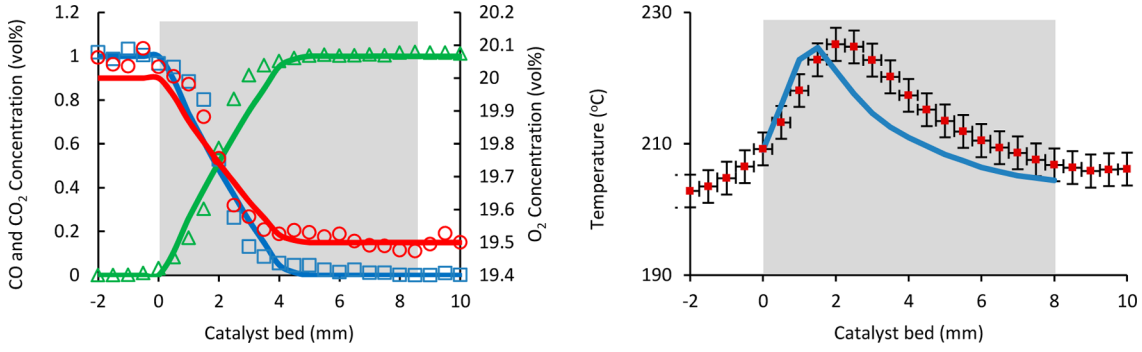

Figure 22. Comparison of experimental (symbols) and fully simulated (solid lines) results of gas-concentration (CO in blue, O_2 in red, and CO_2 in green) and temperature profiles from within a packed powder catalyst bed. Reprinted with permission from ref 149. Copyright 2014 Elsevier.

DOI: 10.1021/acscatal.5b02602
ACS Catal. 2016, 6, 1356−1381

changes in gas concentrations and the nature of surface species, it is still necessary to conduct multiple experiments, with a range of techniques. There have already been recent advances in utilizing more than one technique simultaneously,[20,25,53] while the use of the same sample environment has also been reported for a number of separate characterization techniques (for example XAS and STEM[175]), so as to improve the correlation of data.

Ultimately the major aim of catalytic research, in order to reduce lead times and improve efficiency, would be to conduct simultaneous characterization (using a combination of techniques) under *operando* conditions, and this has to be the next stage for the spatial resolution methodology.

Consequently, there are still a number of opportunities for further development of spatially resolved intracatalyst analysis, and each of these have challenges which must be overcome. For instance, consideration of sample environment that is compatible with multiple analytical techniques is not a trivial matter. Furthermore, if one considers studies of interest to the automotive industry, while SpaciMS and other spectroscopic-based techniques have been applied for intracatalyst and on-engine measurements,[6,7,76,77,176,177] the complications associated with such complex applications with full feedstocks are not necessarily universally resolved for other techniques and all applications; that is, specific technique configurations can have unique sensitivities to particulates and various (e.g., polar, gas-, and liquid-phase) species which must be addressed in the experimental design. These challenges also apply to the kinetic models because, to date, models have mostly been built using model feedstocks, and the response to the added complexity of real feeds is unknown. As such, the kinetic models still require full multi scale validations.

From the current work, the ability of spatial resolution to provide intracatalyst analysis has been established, and the importance of such experimental results to the advancement of modeling is well-justified. As further advances are made (experimentally and theoretically), driven by both the desire to understand catalytic processes along with the benchmarks in automotive emissions legislation (EPA Tier 3, Euro VI, etc.),[178] the full significance of spatially resolved techniques will be realized. Therefore, currently, it is very much a case of "much done but still much more to do"; however, it is clear that substantial progress has been made and that spatially resolved techniques have the potential to contribute to such milestones.

AUTHOR INFORMATION

Corresponding Authors

*E-mail: kmorgan08@qub.ac.uk.
*E-mail: a.goguet@qub.ac.uk.
*E-mail: partridgewp@ornl.gov.

Notes

The authors declare no competing financial interest.

ACKNOWLEDGMENTS

The authors of Queen's University Belfast wish to thank EPSRC UK for funding under the First Grant Scheme (AG; EP/F026390/1), and the CASTech (EP/G02152X/1) and UK Catalysis Hub (EP/K014714/1) projects. Funding of studentships by EPSRC UK and Johnson Matthey under a CASE award (CC), and the Department of Employment and Learning NI (CS) are also acknowledged. W.P.P. thanks Professors William Epling, Michael Harold, Raimund Horn, Petr Kočí, and Louise Olsson, as well as Neal Currier and Melanie DeBusk for helpful discussions. ORNL's research and contributions were sponsored by the U.S. Department of Energy, Office of Energy Efficiency and Renewable Energy, Vehicle Technologies Office, with Gurpreet Singh, Ken Howden, and Leo Breton as the Program Managers. The authors also wish to express gratitude to graphic artist Colby A. Earles of ORNL for the enhancement of the cover art design.

REFERENCES

(1) Hagen, J. Shape-Selective Catalysis: Zeolites. In *Industrial Catalysis: A Practical Approach*; Wiley-VCH Verlag GmbH & Co. KGaA: Weinheim, Germany, 2006; pp 239−259.
(2) Rasmussen, S. B.; Bañares, M. A.; Bazin, P.; Due-Hansen, J.; Ávila, P.; Daturi, M. *Phys. Chem. Chem. Phys.* **2012**, *14*, 2171−2177.
(3) Rothenberg, G. Heterogeneous Catalysis. In *Catalysis: Concepts and Green Applications*; Wiley-VCH Verlag GmbH & Co. KGaA: Weinheim, Germany, 2008; pp 127−187.
(4) Chorkendorff, I., Niemantsverdriet, J. W. Introduction to Catalysis. In *Concepts of Modern Catalysis and Kinetics*; Wiley-VCH Verlag GmbH & Co. KGaA: Weinheim, Germany, 2003; pp 1−21.
(5) Morgan, K. TAP Reactor Development and Application in the Kinetic Characterization of Catalysts for Heterogeneously Catalyzed Gas Phase Reactions. Ph.D. Thesis, Queen's University Belfast, 2010.
(6) Partridge, W. P.; Storey, J. M. E.; Lewis, S. A.; Smithwick, R. W.; DeVault, G. L.; Cunningham, M. J.; Currier, N. V.; Yonushonis, T. M. *SAE Tech. Pap. Ser.* **2000**, Paper no. 2000-01-2952.
(7) Partridge, W. P.; Lewis, S. A.; Ruth, M. J.; Muntean, G. G.; Smith, R. C.; Stang, J. H. *SAE Tech. Pap. Ser.* **2002**, Paper no. 2002-01-2882.
(8) Bentrup, U. *Chem. Soc. Rev.* **2010**, *39*, 4718−4730.
(9) Thibault-Starzyk, F.; Maugé, F. Infrared Spectroscopy. In *Characterization of Solid Materials and Heterogeneous Catalysts: From Structure to Surface Reactivity, Vol. 1&2*; Che, M., Védrine, J. C., Eds.; Wiley-VCH Verlag GmbH & Co. KGaA: Weinheim, Germany, 2012; pp 1−48.
(10) Fan, F.; Feng, Z.; Li, C. Raman and UV-Raman Spectroscopies. In *Characterization of Solid Materials and Heterogeneous Catalysts: From Structure to Surface Reactivity, Vol. 1&2*; Che, M., Védrine, J. C., Eds.; Wiley-VCH Verlag GmbH & Co. KGaA: Weinheim, Germany, 2012; pp 49−87.
(11) Jentoft, F. C. Electronic Spectroscopy: Ultra Violet-Visible and near IR Spectroscopies. In *Characterization of Solid Materials and Heterogeneous Catalysts: From Structure to Surface Reactivity, Vol. 1&2*; Che, M., Védrine, J. C., Eds.; Wiley-VCH Verlag GmbH & Co. KGaA: Weinheim, Germany, 2012; pp 89−147.
(12) Gladden, L. F.; Lutecki, M.; McGregor, J. Nuclear Magnetic Resonance Spectroscopy. In *Characterization of Solid Materials and Heterogeneous Catalysts: From Structure to Surface Reactivity, Vol. 1&2*; Che, M., Védrine, J. C., Eds.; Wiley-VCH Verlag GmbH & Co. KGaA: Weinheim, Germany, 2012; pp 289−342.
(13) Geantet, C.; Pichon, C. X-Ray Absorption Spectroscopy. In *Characterization of Solid Materials and Heterogeneous Catalysts: From Structure to Surface Reactivity, Vol. 1&2*; Che, M., Védrine, J. C., Eds.; Wiley-VCH Verlag GmbH & Co. KGaA: Weinheim, Germany, 2012; pp 511−536.
(14) Behrens, M.; Schlögl, R. X-Ray Diffraction and Small Angle X-Ray Scattering. In *Characterization of Solid Materials and Heterogeneous Catalysts: From Structure to Surface Reactivity, Vol. 1&2*; Che, M.,

DOI: 10.1021/acscatal.5b02602
ACS Catal. 2016, 6, 1356−1381

Védrine, J. C., Eds.; Wiley-VCH Verlag GmbH & Co. KGaA: Weinheim, Germany, 2012; pp 609−653.
(15) Thomas, J. M.; Ducati, C. Transmission Electron Microscopy. In *Characterization of Solid Materials and Heterogeneous Catalysts: From Structure to Surface Reactivity, Vol. 1&2*; Che, M., Védrine, J. C., Eds.; Wiley-VCH Verlag GmbH & Co. KGaA: Weinheim, Germany, 2012; pp 655−701.
(16) Nishino, T.. Scanning Probe Microscopy and Spectroscopy. In *Characterization of Solid Materials and Heterogeneous Catalysts: From Structure to Surface Reactivity, Vol. 1&2*; Che, M., Védrine, J. C., Eds.; Wiley-VCH Verlag GmbH & Co. KGaA: Weinheim, Germany, 2012; pp 703−745.
(17) Alves, S.; Tabet, J.-C. Mass Spectrometry. In *Characterization of Solid Materials and Heterogeneous Catalysts: From Structure to Surface Reactivity, Vol. 1&2*; Che, M., Védrine, J. C., Eds.; Wiley-VCH Verlag GmbH & Co. KGaA: Weinheim, Germany, 2012; pp 881−952.
(18) Bertoncini, F.; Thiebaut, D.; Courtiade, M.; Dutriez, T. Chromatographic Methods. In *Characterization of Solid Materials and Heterogeneous Catalysts: From Structure to Surface Reactivity, Vol. 1&2*; Che, M., Védrine, J. C., Eds.; Wiley-VCH Verlag GmbH & Co. KGaA: Weinheim, Germany, 2012; pp 953−1012.
(19) Efstathiou, A. M.; Gleaves, J. T.; Yablonsky, G. S. Transient Techniques: Temporal Analysis of Products and Steady State Isotopic Transient Kinetic Analysis. In *Characterization of Solid Materials and Heterogeneous Catalysts: From Structure to Surface Reactivity, Vol. 1&2*; Che, M.; Védrine, J. C., Eds.; Wiley-VCH Verlag GmbH & Co. KGaA, Weinheim, Germany, 2012; pp1013−1073.
(20) Beale, A. M.; O'Brien, M. G.; Weckhuysen, B. M. Techniques Coupling for Catalyst Characterisation. In *Characterization of Solid Materials and Heterogeneous Catalysts: From Structure to Surface Reactivity, Vol. 1&2*; Che, M., Védrine, J. C., Eds.; Wiley-VCH Verlag GmbH & Co. KGaA: Weinheim, Germany, 2012; pp 1075−1117.
(21) Perez-Ramirez, J.; Kondratenko, E. V. *Catal. Today* **2007**, *121*, 160−169.
(22) Brant, W. R.; Li, D.; Gu, Q.; Schmid, S. *J. Power Sources* **2016**, *302*, 126−134.
(23) Safonova, O.; Deniau, B.; Millet, J. M. M. *J. Phys. Chem. B* **2006**, *110*, 23962−23967.
(24) Daly, H.; Goguet, A.; Hardacre, C.; Meunier, F. C.; Pilasombat, R.; Thompsett, D. *J. Catal.* **2010**, *273*, 257−265.
(25) Lee, A. F.; Ellis, C. V.; Naughton, J.; Newton, M. A.; Parlett, C. M. A.; Wilson, K. *J. Am. Chem. Soc.* **2011**, *133*, 5724−5727.
(26) Tibiletti, D.; Goguet, A.; Meunier, F. C.; Breen, J. P.; Burch, R. *Chem. Commun.* **2004**, 1636−1637.
(27) Tibiletti, D.; Goguet, A.; Reid, D.; Meunier, F. C.; Burch, R. *Catal. Today* **2006**, *113*, 94−101.
(28) Morgan, K.; Goguet, A.; Hardacre, C. *ACS Catal.* **2015**, *5*, 3430−3445.
(29) Van Santen, R. A.; Sautet, P. Conclusion: Challenges to Computational Catalysis. In *Computational Methods in Catalysis and Materials Science*; Van Santen, R. A., Sautet, P., Eds.; Wiley-VCH Verlag GmbH & Co. KGaA: Weinheim, Germany, 2009; pp 441−446.
(30) McCullough, G.; Douglas, R.; Cunningham, G.; Foley, L. *Proc. Inst. Mech. Eng., Part D* **2001**, *215*, 919−933.
(31) Koltsakis, G. C.; Kandylas, I. P.; Stamatelos, A. M. *Chem. Eng. Commun.* **1998**, *164*, 153−189.
(32) Stewart, J.; Douglas, R.; Goguet, A.; Glover, L. *SAE Tech. Pap. Ser.* **2012**, Paper no. 2012-01-1638.
(33) Stewart, J.; Douglas, R.; Goguet, A. *Proc. Inst. Mech. Eng., Part D* **2014**, *228*, 285−294.
(34) Stewart, J.; Douglas, R.; Goguet, A.; Stere, C. E.; Blades, L. *SAE Tech. Pap. Ser.* **2014**, Paper no. 2014-01-2821.
(35) Pedlow, A.; McCullough, G.; Goguet, A.; Hansen, K. *SAE Tech. Pap. Ser.* **2014**, 2014-01-2814.
(36) Weckhuysen, B. M. *Angew. Chem., Int. Ed.* **2009**, *48*, 4910−4943.
(37) Buurmans, I. L. C.; Weckhuysen, B. M. *Nat. Chem.* **2012**, *4*, 873−886.
(38) Beale, A. M.; Jacques, S. D. M.; Gibson, E. K.; Di Michiel, M. *Coord. Chem. Rev.* **2014**, *277*, 208−223.
(39) Daniel, C.; Clarté, M.-O.; Teh, S.-P.; Thinon, O.; Provendier, H.; Van Veen, A. C.; Beccard, B. J.; Schuurman, Y.; Mirodatos, C. *J. Catal.* **2010**, *272*, 55−64.
(40) Urakawa, A.; Baiker, A. *Top. Catal.* **2009**, *52*, 1312−1322.
(41) Urakawa, A.; Maeda, N.; Baiker, A. *Angew. Chem., Int. Ed.* **2008**, *47*, 9256−9259.
(42) Couves, J. W.; Thomas, J. M.; Waller, D.; Jones, R. H.; Dent, A. J.; Derbyshire, G. E.; Greaves, G. N. *Nature* **1991**, *354*, 465−468.
(43) Clausen, B. S.; Steffensen, G.; Fabius, B.; Villadsen, J.; Feidehhans'l, R.; Topsoe, H. *J. Catal.* **1991**, *132*, 524−535.
(44) Margulies, L.; Kramer, M. J.; McCallum, R. W.; Kycia, S.; Haeffner, D. R.; Lang, J. C.; Goldman, A. *Rev. Sci. Instrum.* **1999**, *70*, 3554−3561.
(45) Eu, W. S.; Cheung, W. H.; Valix, M. *J. Synchrotron Radiat.* **2009**, *16*, 842−848.
(46) Chupas, P. J.; Ciraolo, M. F.; Hanson, J. C.; Grey, C. P. *J. Am. Chem. Soc.* **2001**, *123*, 1694−1702.
(47) Lee, S.; Lee, B.; Seifert, S.; Vajda, S.; Winans, R. E. *Nucl. Instrum. Methods Phys. Res., Sect. A* **2011**, *649*, 200−203.
(48) Grunwaldt, J.-D.; Caravati, M.; Hannemann, S.; Baiker, A. *Phys. Chem. Chem. Phys.* **2004**, *6*, 3037−3047.
(49) Grunwaldt, J.-D.; Baiker, A. *Catal. Lett.* **2005**, *99*, 5−12.
(50) Grunwaldt, J.-D.; Hannemann, S.; Schroer, C. G.; Baiker, A. *J. Phys. Chem. B* **2006**, *110*, 8674−8680.
(51) Zhang, C.; Gustafson, J.; Merte, L. R.; Evertsson, J.; Norén, K.; Carlson, S.; Svensson, H.; Carlsson, P.-A. *Rev. Sci. Instrum.* **2015**, *86*, 1−7.
(52) Gänzler, M. A.; Casapu, M.; Boubnov, A.; Müller, O.; Conrad, S.; Lichtenberg, H.; Frahm, R.; Grunwaldt, J.-D. *J. Catal.* **2015**, *328*, 216−224.
(53) Figueroa, S. J. A.; Newton, M. A. *J. Catal.* **2014**, *312*, 69−77.
(54) O'Brien, M. G.; Beale, A. M.; Jacques, S. D. M.; Di Michiel, M.; Weckhuysen, B. M. *Appl. Catal., A* **2011**, *391*, 468−476.
(55) O'Brien, M. G.; Jacques, S. D. M.; Di Michiel, M.; Barnes, P.; Weckhuysen, B. M.; Beale, A. M. *Chem. Sci.* **2012**, *3*, 509−523.
(56) Wragg, D. S.; O'Brien, M. G.; Bleken, F. L.; Di Michiel, M.; Olsbye, U.; Fjellvåg, H. *Angew. Chem., Int. Ed.* **2012**, *51*, 7956−7959.
(57) Pistidda, C.; Santoru, A.; Garroni, S.; Bergemann, N.; Rzeszutek, A.; Horstmann, C.; Thomas, D.; Klassen, T.; Dornheim, M. *J. Phys. Chem. C* **2015**, *119*, 934−943.
(58) Yuen, E. H. L.; Sederman, A. J.; Gladden, L. F. *Appl. Catal., A* **2002**, *232*, 29−38.
(59) Akpa, B. S.; Mantle, M. D.; Sederman, A. J.; Gladden, L. F. *Chem. Commun.* **2005**, *21*, 2741−2743.
(60) Sederman, A. J.; Mantle, M. D.; Dunckley, C. P.; Huang, Z. Y.; Gladden, L. F. *Catal. Lett.* **2005**, *103*, 1−8.
(61) Gladden, L. F.; Mantle, M. D.; Sederman, A. J. *Adv. Catal.* **2006**, *50*, 1−75.
(62) Nic An tSaoir, M.; Fernandes, D. L. A.; Sá, J.; Kitagawa, K.; Hardacre, C.; Aiouache, F. *Ind. Eng. Chem. Res.* **2012**, *51*, 8875−8882.
(63) Nic An tSaoir, M.; Fernandes, D. L. A.; Sá, J.; McMaster, M.; Kitagawa, K.; Hardacre, C.; Aiouache, F. *Chem. Eng. Sci.* **2011**, *66*, 6407−6423.
(64) Zellner, A.; Suntz, R.; Deutschmann, O. *Angew. Chem., Int. Ed.* **2015**, *54*, 2653−2655.
(65) Matera, S.; Blomberg, S.; Hoffmann, M. J.; Zetterberg, J.; Gustafson, J.; Lundgren, E.; Reuter, K. *ACS Catal.* **2015**, *5*, 4514−4518.
(66) Appel, C.; Mantzaras, J.; Schaeren, R.; Bombach, R.; Inauen, A.; Tylli, N.; Wolf, M.; Griffin, T.; Winkler, D.; Carroni, R. *Proc. Combust. Inst.* **2005**, *30*, 2509−2517.
(67) Schneider, A.; Mantzaras, J.; Bombach, R.; Schenker, S.; Tylli, N.; Jansohn, P. *Proc. Combust. Inst.* **2007**, *31*, 1973−1981.
(68) Titze, T.; Chmelik, C.; Kullmann, J.; Prager, L.; Miersemann, E.; Gläser, R.; Enke, D.; Weitkamp, J.; Kärger, J. *Angew. Chem., Int. Ed.* **2015**, *54*, 5060−5064.
(69) Kundu, P.; Turner, S.; Van Aert, S.; Ravishankar, N.; Van Tendeloo, G. *ACS Nano* **2014**, *8*, 599−606.

DOI: 10.1021/acscatal.5b02602
ACS Catal. 2016, 6, 1356−1381

(70) DeBacker, A.; Martinez, G. T.; MacArthur, K. E.; Jones, L.; Béché, A.; Nellist, P. D.; VanAert, S. *Ultramicroscopy* **2015**, *151*, 56−61.
(71) Baiker, A.; Bergougnan, M. *Can. J. Chem. Eng.* **1985**, *63*, 138−145.
(72) Baiker, A.; Epple, D. *Appl. Catal.* **1986**, *22*, 55−69.
(73) Currier, N. W.; Cunningham, M. J.; Partridge, W. P.; Storey, J. M. E.; Lewis, S. A.; Smithwick, R. W.; DeVault, R. W. Exhaust After-treatment Gas Phase Measurements in situ, 6th Diesel Engine Emissions Reduction Workshop. DEER, 2000, August 23.
(74) Partridge, W. P.; Toops, T. J.; Green, J. B.; Armstrong, T. R. *J. Power Sources* **2006**, *160*, 454−461.
(75) Schwank, J. W.; Tadd, A. R. *Chapter 2: Catalytic reforming of liquid hydrocarbons for on-board solid oxide fuel cell auxiliary power units*; In Catalysis: *Vol. 22*; Spivey, J. J., Dooley, K. M., Eds.; The Royal Society of Chemistry: Cambridge, U.K., 2010; pp 65−67.
(76) West, B.; Huff, S.; Parks, J.; Lewis, S.; Choi, J.-S.; Partridge, W.; Storey, J. *SAE Tech. Pap. Ser.* **2004**, Paper no. 2004-01-3023.
(77) Parks, J.; Huff, S.; Pihl, J.; Choi, J.; West, B. *SAE Tech. Pap. Ser.* **2005**, Paper no. 2005-01-3876.
(78) Choi, J.-S.; Partridge, W. P.; Daw, C. S. *Appl. Catal., A* **2005**, *293*, 24−40.
(79) Choi, J.-S.; Partridge, W. P.; Epling, W. S.; Currier, N. W.; Yonushonis, T. M. *Catal. Today* **2006**, *114*, 102−111.
(80) Choi, J.-S.; Partridge, W. P.; Daw, C. S. *Appl. Catal., B* **2007**, *77*, 145−156.
(81) Choi, J.-S.; Partridge, W. P.; Pihl, J. A.; Daw, C. S. *Catal. Today* **2008**, *136*, 173−182.
(82) Partridge, W. P.; Choi, J. S. *Appl. Catal., B* **2009**, *91*, 144−151.
(83) Cumaranatunge, L.; Mulla, S. S.; Yezerets, A.; Currier, N. W.; Delgass, W. N.; Ribeiro, F. H. *J. Catal.* **2007**, *246*, 29−34.
(84) Shwan, S.; Partridge, W. P.; Choi, J.-S.; Olsson, L. *Appl. Catal., B* **2014**, *147*, 1028−1041.
(85) Choi, J.-S.; Partridge, W. P.; Pihl, J. A.; Kim, M.-Y.; Kočí, P.; Daw, C. S. *Catal. Today* **2012**, *184*, 20−26.
(86) Kočí, P.; Bártová, Š.; Mráček, D.; Marek, M.; Choi, J.-S.; Kim, M.-Y.; Pihl, J. A.; Partridge, W. P. *Top. Catal.* **2013**, *56*, 118−124.
(87) Bártová, Š.; Kočí, P.; Mracek, M.; Pihl, J. A.; Choi, J.-S.; Toops, T. J.; Partridge, W. P. *Catal. Today* **2014**, *231*, 145−154.
(88) Mráček, D.; Kočí, R.; Marek, M.; Choi, J.-S.; Pihl, J. A.; Partridge, W. P. *Appl. Catal., B* **2015**, *166−167*, 509−517.
(89) Stere, C. Development and application of Spaci-MS technique in the investigation of structured catalysts under real reaction conditions. Ph.D. Thesis, Queen's University Belfast, 2012.
(90) Sá, J.; Fernandes, D. L.; Aiouache, F.; Goguet, A.; Hardacre, C.; Lundie, D.; Naeem, W.; Partridge, W. P.; Stere, C. *Analyst* **2010**, *135*, 2260−2272.
(91) http://www.rdmag.com/articles/2010/07/2008-r-d-100-award-winners (accessed April, 11, 2013).
(92) Aftab, K.; Mandur, J.; Budman, H.; Currier, N. W.; Yezerets, A.; Epling, W. S. *Catal. Lett.* **2008**, *125*, 229−235.
(93) Shakir, O.; Yezerets, A.; Currier, N. W.; Epling, W. S. *Appl. Catal., A* **2009**, *365*, 301−308.
(94) Russell, A.; Henry, C.; Currier, N. W.; Yezerets, A.; Epling, W. S. *Appl. Catal., A* **2011**, *397*, 272−284.
(95) Russell, A.; Epling, W. S.; Hess, H.; Chen, H.-Y.; Henry, C.; Currier, N.; Yezerets, A. *Ind. Eng. Chem. Res.* **2010**, *49*, 10311−10322.
(96) Irani, K.; Epling, W. S.; Blint, R. *Top. Catal.* **2009**, *52*, 1856−1859.
(97) Luo, J.-Y.; Hou, X.; Wijayakoon, P.; Schmieg, S. J.; Li, W.; Epling, W. S. *Appl. Catal., B* **2011**, *102*, 110−119.
(98) Luo, J.-Y.; Al-Harbi, M.; Pang, M.; Epling, W. S. *Appl. Catal., B* **2011**, *106*, 664−671.
(99) Hou, X.; Schmieg, S. J.; Li, W.; Epling, W. S. *Catal. Today* **2012**, *197*, 9−17.
(100) Song, X.; Parker, G. G.; Johnson, J. H.; Naber, J. D.; Pihl, J. A. *Emiss. Control Sci. Technol.* **2015**, *1*, 98−107.
(101) Heeb, N. V.; Saxer, C. J.; Forss, A.-M.; Bruhlmann, S. *Atmos. Environ.* **2008**, *42*, 2543−2554.
(102) Chatterjee, D.; Burkhardt, T.; Weibel, M.; Tronconi, E.; Nova, I.; Ciardelli, C. *SAE Tech. Pap. Ser.* **2006**, Paper no. 2006-01-0468.
(103) Epling, W. S. University of Houston, personal communication to W.P.P. 2015.
(104) Olsson, L. Chalmers University of Technology, personal communication to W.P.P. 2015.
(105) Chemistry WebBook; http://webbook.nist.gov/chemistry/form-ser.html (accessed August 18, 2015.
(106) Bosco, M.; Vogel, F. *Catal. Today* **2006**, *116*, 348−353.
(107) Kopyscinski, J.; Schildhauer, T. J.; Vogel, F.; Biollaz, S. M. A.; Wokaun, A. *J. Catal.* **2010**, *271*, 262−279.
(108) Diehm, C.; Karadeniz, H.; Karakaya, C.; Hettel, M.; Deutschmann, O. *Adv. Chem. Eng.* **2014**, *45*, 41−95.
(109) Roos, M.; Bansmann, J.; Zhang, D.; Deutschmann, O.; Behm, R. J. *J. Chem. Phys.* **2010**, *133*, 1−11.
(110) Roos, M.; Kielbassa, S.; Schirling, C.; Häring, T.; Bansmann, J.; Behm, R. J. *Rev. Sci. Instrum.* **2007**, *78*, 1−9.
(111) Johansson, M.; Hoffmann Jørgensen, J.; Chorkendorff, I. *Rev. Sci. Instrum.* **2004**, *75*, 2082−2093.
(112) Bugosh, G. S.; Easterling, V. G.; Rusakova, I. A.; Harold, M. P. *Appl. Catal., B* **2015**, *165*, 68−78.
(113) Hettel, M.; Diehm, C.; Torkashvand, B.; Deutschmann, O. *Catal. Today* **2013**, *216*, 2−10.
(114) Diehm, C.; Deutschmann, O. *Int. J. Hydrogen Energy* **2014**, *39*, 17998−18004.
(115) Chan, D.; Tischer, S.; Heck, J.; Diehm, C.; Deutschmann, O. *Appl. Catal., B* **2014**, *156−157*, 153−165.
(116) Korup, O.; Mavlyankariev, S.; Geske, M.; Goldsmith, C. F.; Horn, R. *Chem. Eng. Process.* **2011**, *50*, 998−1009.
(117) Horn, R.; Williams, K. A.; Degenstein, N. J.; Schmidt, L. D. *J. Catal.* **2006**, *242*, 92−102.
(118) Dalle Nogare, D.; Degenstein, N. J.; Horn, R.; Canu, P.; Schmidt, L. D. *J. Catal.* **2008**, *258*, 131−142.
(119) Nogare, D. D.; Degenstein, N. J.; Horn, R.; Canu, P.; Schmidt, L. D. *J. Catal.* **2011**, *277*, 134−148.
(120) Horn, R.; Degenstein, N. J.; Williams, K. A.; Schmidt, L. D. *Catal. Lett.* **2006**, *110*, 169−178.
(121) Horn, R.; Williams, K. A.; Degenstein, N. J.; Schmidt, L. D. *Chem. Eng. Sci.* **2007**, *62*, 1298−1307.
(122) Horn, R.; Williams, K. A.; Degenstein, N. J.; Bitsch-Larsen, A.; Dalle Nogare, D.; Tupy, S. A.; Schmidt, L. D. *J. Catal.* **2007**, *249*, 380−393.
(123) Donazzi, A.; Michael, B. C.; Schmidt, L. D. *J. Catal.* **2008**, *260*, 270−275.
(124) Bitsch-Larsen, A.; Horn, R.; Schmidt, L. D. *Appl. Catal., A* **2008**, *348*, 165−172.
(125) Horn, R.; Korup, O.; Geske, M.; Zavyalova, U.; Oprea, I.; Schlögl, R. *Rev. Sci. Instrum.* **2010**, *81*, 064102−064109.
(126) Michael, B. C.; Nare, D. N.; Schmidt, L. D. *Chem. Eng. Sci.* **2010**, *65*, 3893−3902.
(127) Horn, R. International Patent WO 2011/072701 A1, 2011.
(128) Korup, O.; Schlogl, R.; Horn, R. *Catal. Today* **2012**, *181*, 177−183.
(129) Geske, M.; Korup, O.; Horn, R. *Catal. Sci. Technol.* **2013**, *3*, 169−175.
(130) Korup, O.; Goldsmith, C. F.; Weinberg, G.; Geske, M.; Kandemir, T.; Schlögl, R.; Horn, R. *J. Catal.* **2013**, *297*, 1−16.
(131) Horn, R. Hamburg University of Technology, personal communication to W.P.P. 2015.
(132) Beretta, A.; Donazzi, A.; Livio, D.; Maestri, M.; Groppi, G.; Tronconi, E.; Forzatti, P. *Catal. Today* **2011**, *171*, 79−83.
(133) Donazzi, A.; Maestri, M.; Michael, B. C.; Beretta, A.; Forzatti, P.; Groppi, G.; Tronconi, E.; Schmidt, L. D.; Vlachos, D. G. *J. Catal.* **2010**, *275*, 270−279.
(134) Donazzi, A.; Livio, D.; Maestri, M.; Beretta, A.; Groppi, G.; Tronconi, E.; Forzatti, P. *Angew. Chem., Int. Ed.* **2011**, *50*, 3943−3946.
(135) Donazzi, A.; Livio, D.; Beretta, A.; Groppi, G.; Forzatti, P. *Appl. Catal., A* **2011**, *402*, 41−49.

DOI: 10.1021/acscatal.5b02602
ACS Catal. 2016, 6, 1356−1381

(136) Livio, D.; Donazzi, A.; Beretta, A.; Groppi, G.; Forzatti, P. *Top. Catal.* **2011**, *54*, 866−872.
(137) Livio, D.; Diehm, C.; Donazzi, A.; Beretta, A.; Deutschmann, O. *Appl. Catal., A* **2013**, *467*, 530−541.
(138) Donazzi, A.; Livio, D.; Diehm, C.; Beretta, A.; Groppi, G.; Forzatti, P. *Appl. Catal., A* **2014**, *469*, 52−64.
(139) Allison, S. W.; Gillies, G. T. *Rev. Sci. Instrum.* **1997**, *68*, 2615−2650.
(140) Khalid, A. H.; Kontis, K. *Sensors* **2008**, *8*, 5673−5744.
(141) Kersey, A. D.; Davis, M. A.; Patrick, H. J.; LeBlanc, M.; Koo, K. P.; Askins, C. G.; Putnam, M. A.; Friebele, E. J. *J. Lightwave Technol.* **1997**, *15*, 1442−1463.
(142) Soller, B. J.; Gifford, D. K.; Wolfe, M. S.; Froggatt, M. E. *Opt. Express* **2005**, *13*, 666−674.
(143) Mussi, G.; Gisin, N.; Passy, R.; von der Weid, J. P. *Electron. Lett.* **1996**, *32*, 926−927.
(144) Nguyen, H.; Harold, M. P.; Luss, D. *Chem. Eng. J.* **2013**, *234*, 312−317.
(145) Nguyen, H.; Harold, M. P.; Luss, D. *Chem. Eng. J.* **2015**, *262*, 464−477.
(146) Touitou, J. Development of an in situ spatially resolved technique to investigate catalysts in a plug flow reactor. Ph.D. Thesis, Queen's University Belfast, 2014.
(147) Touitou, J.; Morgan, K.; Burch, R.; Hardacre, C.; Goguet, A. *Catal. Sci. Technol.* **2012**, *2*, 1811−1813.
(148) Touitou, J.; Burch, R.; Hardacre, C.; McManus, C.; Morgan, K.; Sá, J.; Goguet, A. *Analyst* **2013**, *138*, 2858−2862.
(149) Touitou, J.; Aiouache, F.; Burch, R.; Douglas, R.; Hardacre, C.; Morgan, K.; Sá, J.; Stewart, C.; Stewart, J.; Goguet, A. *J. Catal.* **2014**, *319*, 239−246.
(150) Goguet, A.; Partridge, W. P.; Aiouche, F.; Hardacre, C.; Morgan, K.; Sá, J.; Stere, C. *Catal. Today* **2014**, *236*, 206−208.
(151) Partridge, W. P.; Currier, N.; Kim, M.-Y.; Pihl, J. A.; Connatser, R. M.; Choi, J.-S.; Yezerets, A.; Kamasamudram, K. Cummins/ORNL FEERC Combustion CRADA: NOx Control & Measurement Technology for Heavy-Duty Diesel Engines, Self-Diagnosing Smart-Catalyst Systems, 2014 DOE Vehicle Technologies Program Annual Merit Review, Washington, D.C., June 19, 2014. http://energy.gov/sites/prod/files/2014/07/f17/ace032_partridge_2014_o.pdf (accessed August 18, 2015).
(152) Kim, M.-Y.; Choi, J.-S.; Partridge, W. P. Unpublished original data, Oak Ridge National Laboratory, 2015.
(153) Nguyen, H.; Harold, M. P.; Luss, D. Oral presentation O-F-408-3. A Study on Spatiotemporal Temperature and Concentration Measurements in Monolith Reactor, 24th North American Catalysis Society Meeting 2015.
(154) Harold, M.; University of Houston, personal communication to WPP, 2015, intended for publication.
(155) Hettel, M.; Diehm, C.; Deutschmann, O. *Catal. Today* **2014**, *236*, 209−213.
(156) Sjoblom, J. Parameter estimation in heterogeneous catalysis. Ph.D. thesis, Chalmers University of Technology, 2009.
(157) Ansell, G. P.; Bennett, P. S.; Cox, J. P.; Frost, J. C.; Gray, P. G.; Jones, A.-M.; Rajaram, R. R.; Walker, A. P.; Litorell, M.; Smedler, G. *Appl. Catal., B* **1996**, *10*, 183−201.
(158) Auvray, X.; Partridge, W. P.; Choi, J.-S.; Pihl, J. A.; Yezerets, A.; Kamasamudram, K.; Currier, N. W.; Olsson, L. *Appl. Catal., B* **2012**, *126*, 144−152.
(159) Auvray, X.; Partridge, W. P.; Choi, J.-S.; Pihl, J. A.; Coehlo, F.; Yezerets, A.; Kamasamudram, K.; Currier, N. W.; Olsson, L. *Appl. Catal., B* **2015**, *163*, 393−403.
(160) Leskovjan, M.; Mrácek, D.; Kocí, P. *Proceedings of the 41st International Conference of Slovak Society of Chemical Engineering*, Tatranské Matliare, Slovakia, May 23−27, 2014; pp 743−749.
(161) Mráček, D.; Kočí, R.; Choi, J.-S.; Partridge, W. P. *Appl. Catal., B* **2016**, *182*, 109−114.
(162) Maestri, M.; Beretta, A.; Groppi, G.; Tronconi, E.; Forzatti, P. *Catal. Today* **2005**, *105*, 709−717.
(163) Tavazzi, I.; Maestri, M.; Beretta, A.; Groppi, G.; Tronconi, E.; Forzatti, P. *AIChE J.* **2006**, *52*, 3234−3245.
(164) Mhadeshwar, A. B.; Wang, H.; Vlachos, D. G. *J. Phys. Chem. B* **2003**, *107*, 12721−12733.
(165) Quiceno, R.; Peréz-Ramírez, J.; Warnatz, J.; Deutschmann, O. *Appl. Catal., A* **2006**, *303*, 166−176.
(166) Koop, J.; Deutschmann, O. *Appl. Catal., B* **2009**, *91*, 47−58.
(167) Mhadeshwar, A. B.; Vlachos, D. G. *Ind. Eng. Chem. Res.* **2007**, *46*, 5310−5324.
(168) Hauptmann, W.; Votsmeier, M.; Vogel, H.; Vlachos, D. G. *Appl. Catal., A* **2011**, *397*, 174−182.
(169) Hettel, M.; Diehm, C.; Bonart, H.; Deutschmann, O. *Catal. Today* **2015**, *258*, 230−240.
(170) Wehinger, G. D.; Heitmann, H.; Kraume, M. *Chem. Eng. J.* **2016**, *284*, 543−556.
(171) Wehinger, G. D.; Eppinger, T.; Kraume, M. *Chem. Eng. Sci.* **2014**, *111*, 220−230.
(172) Wehinger, G. D.; Eppinger, T.; Kraume, M. *Chem. Eng. Sci.* **2015**, *122*, 197−209.
(173) Voltz, S. E.; Morgan, C. R.; Liederman, D.; Jacob, S. M. *Ind. Eng. Chem. Prod. Res. Dev.* **1973**, *12*, 294−301.
(174) Stewart, J.; Douglas, R.; Goguet, A.; Stere, C. *Can. J. Chem. Eng.* **2014**, *92*, 1535−1541.
(175) Li, Y.; Zakharov, D.; Zhao, S.; Tappero, R.; Jung, U.; Elsen, A.; Baumann, P.; Nuzzo, R. G.; Stach, E. A.; Frenkel, A. I. *Nat. Commun.* **2015**, *6*, 1−6.
(176) Yoo, J.; Prikhodko, V.; Parks, J. E.; Perfetto, A.; Geckler, S.; Partridge, W. P. *Appl. Spectrosc.* **2015**, *69*, 1047−1058.
(177) Yoo, J.; Prikhodko, V.; Parks, J. E.; Perfetto, A.; Geckler, S.; Partridge, W. P. *Appl. Spectrosc.* **2015**, *69*, 1047−1058.
(178) Johnson, T. V. *SAE Int. J. Engines* **2015**, *8*, Paper no. 2015-01-0993.

DOI: 10.1021/acscatal.5b02602
ACS Catal. 2016, 6, 1356−1381